CpG islands was significantly higher in Cluster B_T based on BAMCA than in Cluster A_T. The frequency of CIMP in Cluster B_T was significantly higher than that in Cluster A_T. Genome-wide DNA methylation alterations consisting of both hypo- and hypermethylation revealed by BAMCA in Cluster B_T were associated with regional DNA hypermethylation of C-type CpG islands. For comparison with their DNA methylation status, we also examined copy number alterations by array-based comparative genomic hybridization. By unsupervised hierarchical clustering analysis based on copy number alterations, RCCs were clustered into the two subclasses, clusters A_{TG} and B_{TG}. Loss of chromosome 3p and gain of chromosomes 5q and 7 were frequent in both clusters A_{TG} and B_{TG}. Loss of chromosomes 1p, 4, 9, 13q, and 14q was frequent only in Cluster B_{TG}, and not in Cluster A_{TG}.[74] RCCs showing higher histological grades, renal vein tumor thrombi, vascular involvement and higher pathological TNM stages were accumulated in Cluster B_{TG}. The recurrence-free and overall survival rates of patients in Cluster B_{TG} were significantly lower than those of patients in Cluster A_{TG}.[74] A subclass of Cluster B_T based on BAMCA data was completely included in Cluster B_{TG} showing accumulation of copy number alterations. Genetic and epigenetic alterations are not mutually exclusive during renal carcinogenesis, and particular DNA methylation profiles may be closely related to chromosomal instability. DNA methylation alterations at the precancerous stage, which may not occur randomly but may foster further epigenetic and genetic alterations, can generate more malignant cancers and even determine patient outcome (Fig. 3).

Carcinogenetic risk estimation and prognostication based on DNA methylation status. In samples of non-cancerous liver tissue obtained from patients with HCCs, many BAC clones show DNA hypo- or hypermethylation in comparison with normal liver tissue from patients without HCCs (Fig. 4a).[75] The effectiveness of surgical resection for HCC is limited, unless the disease is diagnosed early at the asymptomatic stage. Therefore, surveillance at the precancerous stage is a priority for patients with HBV or HCV infection. To reveal the baseline liver histology, microscopic examination of liver biopsy specimens is carried out in patients with HBV or HCV infection prior to interferon therapy.[76,77] Carcinogenetic risk estimation using such liver biopsy specimens is advantageous for close follow-up of patients who are at high risk of HCC development. To establish an indicator for carcinogenetic risk estimation, we first omitted potentially insignificant BAC clones associated only with inflammation and/or fibrosis and focused on BAC clones for which DNA methylation status was altered at the precancerous stage in comparison to normal liver tissue and was inherited by HCCs themselves from the precancerous stage (Fig. 4b). Among the BAC clones studied, a bioinformatics approach further identified the top 25 for which DNA methylation status was able to discriminate non-cancerous liver tissue from patients with HCCs in the learning cohort from normal liver tissue with sufficient sensitivity and specificity.[75] By two-dimensional hierarchical clustering analysis using these 25 BAC clones, samples of normal liver tissue and samples of non-cancerous liver tissue obtained from patients with HCCs in the learning cohort were successfully subclassified into different subclasses without any error (Fig. 4c). The criteria established using a combination of the DNA methylation status of the 25 BAC clones (Fig. 4d) diagnosed non-cancerous liver tissue from patients with HCCs in the learning cohort as being at high risk of carcinogenesis with a sensitivity and specificity of 100%.[75] The sensitivity and specificity in the validation cohort were both 96%, and thus our criteria were successfully validated.[75]

It was confirmed that there were no significant differences in the number of BAC clones satisfying our criteria between samples of non-cancerous liver tissue showing chronic hepatitis and samples of non-cancerous liver tissue showing cirrhosis, indicating that our criteria were not associated with the degree of inflammation or fibrosis.[75] In addition, the average numbers of BAC clones satisfying our criteria were significantly lower in liver tissue samples from patients with HBV or HCV infection but without HCCs than in samples of non-cancerous liver tissue obtained from patients with HCCs.[75] Therefore, our criteria may be applicable for classifying liver tissue samples obtained from patients who are being followed up because of HBV or HCV infection, chronic hepatitis, or cirrhosis into those that may generate HCCs and those that will not. We intend to validate the reliability of such risk estimation prospectively using liver biopsy specimens obtained prior to interferon therapy from a large cohort of patients with HBV or HCV infection.

To establish criteria for prognostication of patients with HCCs, in the learning cohort, patients who had survived more than 4 years after hepatectomy and patients who had suffered recurrence within 6 months and died within a year after hepatectomy were defined as a favorable-outcome group and a poor-outcome group, respectively. Wilcoxon test revealed that the signal ratios of 41 BAC clones differed significantly between the two groups.[75] Two-dimensional hierarchical clustering analysis using the 41 BAC clones successfully subclassified HCCs in the favorable-outcome group and the poor-outcome group into different subclasses without any error (Fig. 5a). We also established cut-off values for the 41 BAC clones that allowed discrimination of samples between the poor-outcome and favorable-outcome groups with sufficient sensitivity and specificity (Fig. 5b). Multivariate analysis revealed that satisfying our criteria for 32 or more BAC clones was a predictor of overall patient outcome and was independent of parameters that are already known to have prognostic significance,[75] such as histological differentiation, and presence of portal vein tumor thrombi, intrahepatic metastasis, and multicentricity.[33] The cancer-free and overall survival rates of patients with HCCs satisfying the criteria for 32 or more BAC clones in the validation cohort were significantly lower than those of patients with HCCs satisfying the criteria for less than 32 BAC clones (Fig. 5c).[75] Such prognostication using liver biopsy specimens obtained before transarterial embolization, transarterial chemoembolization, and radiofrequency ablation may be advantageous even for patients who undergo such therapies.

As mentioned above, even non-cancerous urothelia showing no remarkable histological changes obtained from patients with UCs may be exposed to carcinogens in urine. In fact, genome-wide DNA methylation profiles of non-cancerous urothelia obtained from patients with nodular invasive UCs showing an aggressive clinical course were inherited by the nodular invasive UCs themselves, suggesting that DNA methylation alterations that were correlated with the development of more malignant invasive cancers had already accumulated in non-cancerous urothelia.[78] These findings prompted us to estimate the degree of carcinogenetic risk based on DNA methylation profiles in non-cancerous urothelia. We were able to identify BAC clones for which DNA methylation status was able to completely discriminate non-cancerous urothelia from patients with UCs from normal urothelia and diagnose them as having a high risk of urothelial carcinogenesis.[78] If it were possible to identify individuals who are at high risk of urothelial carcinogenesis, then strategies for the prevention or early detection of UCs, such as smoking cessation or repeated urine cytology examinations, might be applicable.

In order to start adjuvant systemic chemotherapy immediately in patients who have undergone total cystectomy and are still at high risk of recurrence and metastasis of UCs, prognostic indicators have been explored. Subclassification based on unsupervised two-dimensional hierarchical clustering analysis using BAMCA data for UCs was significantly correlated with recurrence after surgery due to metastasis to pelvic lymph nodes or

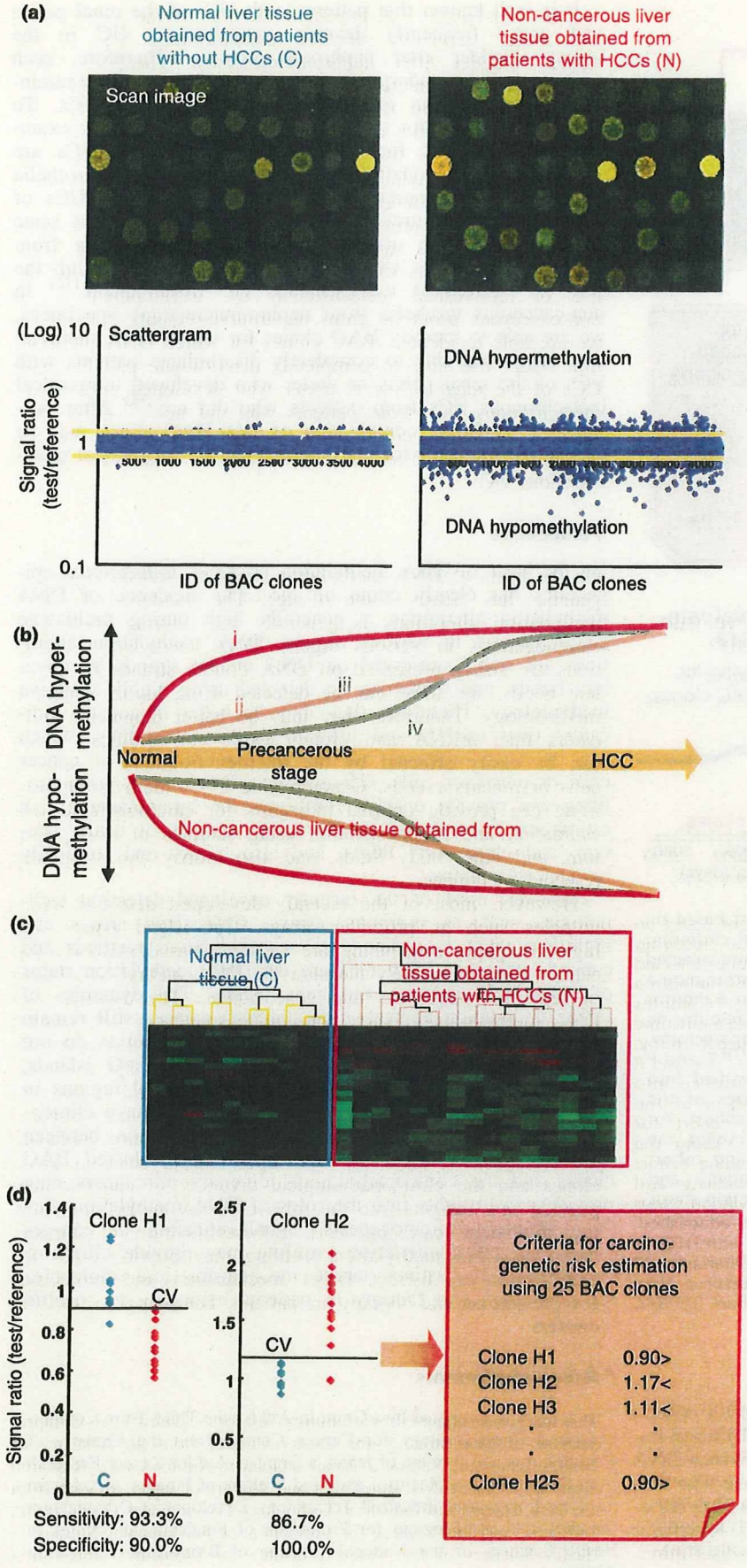

Fig. 4. Risk estimation of hepatocellular carcinoma (HCC) development based on DNA methylation status. (a) Examples of scan images and scattergrams of signal ratios in normal liver tissue obtained from patients without HCCs (C) and non-cancerous liver tissue obtained from patients with HCCs (N). In N samples, many bacterial artificial chromosome (BAC) clones showed DNA hypo- or hypermethylation compared to C samples.[75] (b) Four patterns of DNA methylation alterations seen in BAC clones during multistage hepatocarcinogenesis: (i) DNA methylation alterations occurred at the chronic hepatitis and liver cirrhosis stage, and DNA methylation status did not alter in HCCs from the chronic hepatitis and liver cirrhosis stage; (ii) DNA methylation alterations occurred at the chronic hepatitis and liver cirrhosis stage and further altered in HCCs; (iii) although DNA methylation alterations occurred at the chronic hepatitis and liver cirrhosis stage, the DNA methylation status returned to normal in HCCs; and (iv) DNA methylation alterations occurred only in HCCs. In order to establish criteria for carcinogenetic risk estimation, we focused on BAC clones whose DNA methylation status was inherited by HCCs from the precancerous stage (groups i and ii), whereas group iii may only reflect inflammation and/or fibrosis, and group iv may participate only in the malignant progression stage. (c) Two-dimensional hierarchical clustering analysis using BAC clones that were selected as the top 25 for which DNA methylation status was able to discriminate N from C with sufficient sensitivity and specificity by Wicoxon test and the support vector machine algorithm.[75] C and N samples in the learning cohort were successfully subclassified into different subclasses without any error.[75] (d) Scattergrams of the signal ratios in C and N samples in the learning cohort for representative BAC clones, Clone H1 and Clone H2. Using the cut-off values (CV) in each panel, N samples in the learning cohort were discriminated from C samples with sufficient sensitivity and specificity.[75] Based on a combination of DNA methylation status for the 25 BAC clones, the criteria for carcinogenetic risk estimation were established. Using these criteria, the sensitivity and specificity for diagnosis of N samples in the learning cohort as being at high risk of carcinogenesis were both 100%.[75] The sensitivity and specificity in the validation cohort were both 96%, and thus the criteria were successfully validated.[75]

doi: 10.1111/j.1349-7006.2009.01383.x

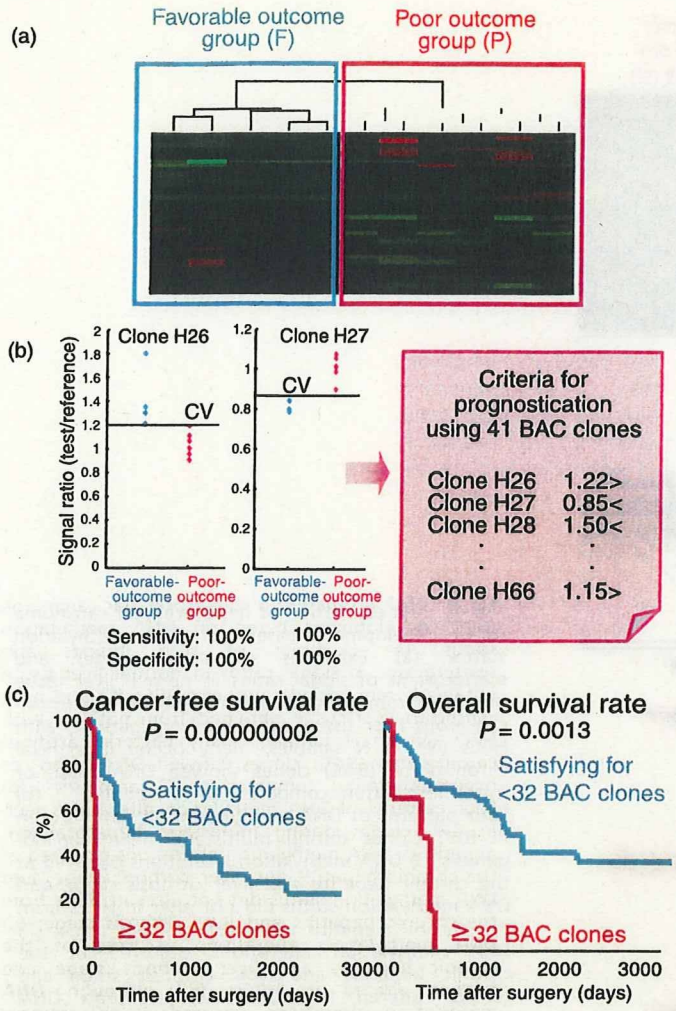

Fig. 5. Prognostication of patients with HCC development based on DNA methylation status. (a) Two-dimensional hierarchical clustering analysis using 41 bacterial artificial chromosome (BAC) clones selected as those for which DNA methylation status was able to discriminate a poor-outcome group (P), who suffered recurrence within 6 months and died within a year after hepatectomy, from a favorable-outcome group (F), who survived for more than 4 years after hepatectomy, with sufficient sensitivity and specificity by Wilcoxon test.[75] F and P patients in the learning cohort were successfully subclassified into different subclasses without any error.[75] (b) Scattergrams of the signal ratios in F and P patients in the learning cohort for representative BAC clones, Clone H26 and Clone H27. Using the cut-off values (CV) in each panel, P patients in the learning cohort were discriminated from F patients with 100% sensitivity and specificity.[75] Based on a combination of the DNA methylation status of the 41 BAC clones, criteria for prognostication were established. (c) The cancer-free and overall survival rates of patients with HCCs in the validation cohort. Patients with HCCs satisfying the criteria for 32 or more BAC clones showed significantly poorer outcome than patients with HCCs satisfying the criteria for less than 32 BAC clones.[75]

distant organs.[78] These data prompted us to establish criteria for predicting recurrence of UCs based on DNA methylation status, and we successfully identified BAC clones for which DNA methylation status completely discriminated patients who suffered recurrence from patients who did not, whereas high histological grade, invasive growth, and vascular or lymphatic involvement were unable to achieve such complete discrimination.[78]

It is well known that patients with UCs of the renal pelvis and ureter frequently develop metachronous UC in the urinary bladder after nephroureterectomy. Therefore, such patients need to undergo repeated urethrocystoscopic examinations for detection of intravesical metachronous UCs. To decrease the need for such invasive urethrocystoscopic examinations, indicators for intravesical metachronous UCs are needed. DNA methylation profiles of non-cancerous urothelia obtained by nephroureterectomy from patients with UCs of the renal pelvis or ureter, which may be exposed to the same carcinogens in the urine as non-cancerous urothelia from which metachronous UCs originate, were correlated with the risk of intravesical metachronous UC development.[78] In non-cancerous urothelia from nephroureterectomy specimens, we are able to identify BAC clones for which DNA methylation status was able to completely discriminate patients with UCs of the renal pelvis or ureter who developed intravesical metachronous UCs from patients who did not.[78] After prospective validation, combination of such BAC clones may be an optimal indicator for the development of intravesical metachronous UC.

Perspective

On the basis of DNA methylation profiling, translational epigenetics has clearly come of age. The incidence of DNA methylation alterations is generally high during multistage carcinogenesis in various organs. DNA methylation alterations are stably preserved on DNA double strands by covalent bonds, and these can be detected using highly sensitive methodology. Therefore, they may be better diagnostic indicators than mRNA and protein expression profiles, which can be easily affected by the microenvironment of cancer cells or precursor cells. Genome-wide DNA methylation profiling can provide optimal indicators for carcinogenetic risk estimation and prognostication using samples of urine, sputum, and other body fluids, and also biopsy and surgically resected specimens.

However, most of the recently developed detection technologies such as promoter arrays, CpG-island arrays and high-throughput sequencing are sequence-based methods and cannot comprehensively measure the DNA methylation status of repetitive sequences and gene bodies. The dynamics of DNA methylation at such non-unique sequences still remain to be determined.[79] Our BAC array-based methods do not focus only on specific promoter regions and CpG islands, and have successfully identified the chromosomal regions in which coordinated DNA methylation alterations have clinicopathological impact. Evaluation of the correlation between the methylation status of each CpG site in selected BAC clones and the clinicopathological diversity of cancers may provide new insights into the roles of DNA methylation during multistage carcinogenesis. Subclassification of cancers based on DNA methylation profiling may provide clues for clarification of distinct target mechanisms and molecules for prevention and therapy in patients belonging to specific clusters.

Acknowledgments

This study was supported by a Grant-in-Aid for the Third Term Comprehensive 10-Year Strategy for Cancer Control from the Ministry of Health, Labor and Welfare of Japan, a Grant-in-Aid for Cancer Research from the Ministry of Health, Labor and Welfare of Japan, a Grant from the New Energy and Industrial Technology Development Organization (NEDO), and the Program for Promotion of Fundamental Studies in Health Sciences of the National Institute of Biomedical Innovation (NiBio).

Abbreviations

BAC	bacterial artificial chromosome
BAMCA	BAC array-based methylated CpG island amplification
CIMP	CpG island methylator phenotype
DNMT	DNA methyltransferase
HBV	hepatitis B virus
HCC	hepatocellular carcinoma
HCV	hepatitis C virus
LOH	loss of heterozygosity
PanIN	pancreatic intraductal neoplasia
PCNA	proliferating cell nuclear antigen
RCC	renal cell carcinoma
UC	urothelial carcinoma

References

1 Delcuve GP, Rastegar M, Davie JR. Epigenetic control. *J Cell Physiol* 2009; **219**: 243–50.
2 Hermann A, Gowher H, Jeltsch A. Biochemistry and biology of mammalian DNA methyltransferases. *Cell Mol Life Sci* 2004; **61**: 2571–87.
3 Bestor T, Laudano A, Mattaliano R, Ingram V. Cloning and sequencing of a cDNA encoding DNA methyltransferase of mouse cells. The carboxyl-terminal domain of the mammalian enzymes is related to bacterial restriction methyltransferases. *J Mol Biol* 1988; **203**: 971–83.
4 Chuang LS, Ian HI, Koh TW, Ng HH, Xu G, Li BF. Human DNA-(cytosine-5) methyltransferase-PCNA complex as a target for p21WAF1. *Science* 1997; **277**: 1996–2000.
5 Baylin SB. Tying it all together: epigenetics, genetics, cell cycle, and cancer. *Science* 1997; **277**: 1948–9.
6 Bestor TH. The DNA methyltransferases of mammals. *Hum Mol Genet* 2000; **9**: 2395–402.
7 Okano M, Bell DW, Haber DA, Li E. DNA methyltransferases Dnmt3a and Dnmt3b are essential for de novo methylation and mammalian development. *Cell* 1999; **99**: 247–57.
8 Cedar H, Bergman Y. Linking DNA methylation and histone modification: patterns and paradigms. *Nat Rev Genet* 2009; **10**: 295–304.
9 Jones PL, Veenstra GJ, Wade PA *et al.* Methylated DNA and MeCP2 recruit histone deacetylase to repress transcription. *Nat Genet* 1998; **19**: 187–91.
10 Nan X, Ng HH, Johnson CA *et al.* Transcriptional repression by the methyl-CpG-binding protein MeCP2 involves a histone deacetylase complex. *Nature* 1998; **393**: 386–9.
11 Kanai Y, Ushijima S, Nakanishi Y, Hirohashi S. Reduced mRNA expression of the DNA demethylase, MBD2, in human colorectal and stomach cancers. *Biochem Biophys Res Commun* 1999; **264**: 962–6.
12 Esteve PO, Chin HG, Smallwood A *et al.* Direct interaction between DNMT1 and G9a coordinates DNA and histone methylation during replication. *Genes Dev* 2006; **20**: 3089–103.
13 Fuks F, Hurd PJ, Deplus R, Kouzarides T. The DNA methyltransferases associate with HP1 and the SUV39H1 histone methyltransferase. *Nucleic Acids Res* 2003; **31**: 2305–12.
14 Suzuki MM, Bird A. DNA methylation landscapes: provocative insights from epigenomics. *Nat Rev Genet* 2008; **9**: 465–76.
15 Laird PW, Jackson-Grusby L, Fazeli A *et al.* Suppression of intestinal neoplasia by DNA hypomethylation. *Cell* 1995; **81**: 197–205.
16 Eden A, Gaudet F, Waghmare A, Jaenisch R. Chromosomal instability and tumors promoted by DNA hypomethylation. *Science* 2003; **300**: 455.
17 Yoshiura K, Kanai Y, Ochiai A, Shimoyama Y, Sugimura T, Hirohashi S. Silencing of the E-cadherin invasion-suppressor gene by CpG methylation in human carcinomas. *Proc Natl Acad Sci USA* 1995; **92**: 7416–9.
18 Jones PA, Baylin SB. The fundamental role of epigenetic events in cancer. *Nat Rev Genet* 2002; **3**: 415–28.
19 Baylin SB, Ohm JE. Epigenetic gene silencing in cancer – a mechanism for early oncogenic pathway addiction? *Nat Rev Cancer* 2006; **6**: 107–16.
20 Gronbaek K, Hother C, Jones PA. Epigenetic changes in cancer. *Apmis* 2007; **115**: 1039–59.
21 Jones PA, Baylin SB. The epigenomics of cancer. *Cell* 2007; **128**: 683–92.
22 Esteller M. Epigenetics in cancer. *N Engl J Med* 2008; **358**: 1148–59.
23 Shibata D. Inferring human stem cell behaviour from epigenetic drift. *J Pathol* 2009; **217**: 199–205.
24 Ohm JE, McGarvey KM, Yu X *et al.* A stem cell-like chromatin pattern may predispose tumor suppressor genes to DNA hypermethylation and heritable silencing. *Nat Genet* 2007; **39**: 237–42.
25 Pogribny IP, Beland FA. DNA hypomethylation in the origin and pathogenesis of human diseases. *Cell Mol Life Sci* 2009; **66**: 2249–61.
26 Laird PW. The power and the promise of DNA methylation markers. *Nat Rev Cancer* 2003; **3**: 253–66.
27 Issa JP, Kantarjian HM. Targeting DNA methylation. *Clin Cancer Res* 2009; **15**: 3938–46.
28 Kanai Y, Hirohashi S. Alterations of DNA methylation associated with abnormalities of DNA methyltransferases in human cancers during transition from a precancerous to a malignant state. *Carcinogenesis* 2007; **28**: 2434–42.
29 Kanai Y. Alterations of DNA methylation and clinicopathological diversity of human cancers. *Pathol Int* 2008; **58**: 544–58.
30 Tsuda H, Zhang WD, Shimosato Y *et al.* Allele loss on chromosome 16 associated with progression of human hepatocellular carcinoma. *Proc Natl Acad Sci USA* 1990; **87**: 6791–4.
31 Kanai Y, Ushijima S, Tsuda H, Sakamoto M, Sugimura T, Hirohashi S. Aberrant DNA methylation on chromosome 16 is an early event in hepatocarcinogenesis. *Jpn J Cancer Res* 1996; **87**: 1210–7.
32 Kanai Y, Ushijima S, Tsuda H, Sakamoto M, Hirohashi S. Aberrant DNA methylation precedes loss of heterozygosity on chromosome 16 in chronic hepatitis and liver cirrhosis. *Cancer Lett* 2000; **148**: 73–80.
33 Hirohashi S, Ishak KG, Kojiro M *et al.* Hepatocellular carcinoma. In: Hamilton SR, Altonen LA, eds. *World Health Organization classification of tumours. Pathology and genetics. Tumours of the digestive system.* Lyon: IARC Press, 2000; 159–72.
34 Hirohashi S, Kanai Y. Cell adhesion system and human cancer morphogenesis. *Cancer Sci* 2003; **94**: 575–81.
35 Kanai Y, Ushijima S, Hui AM *et al.* The E-cadherin gene is silenced by CpG methylation in human hepatocellular carcinomas. *Int J Cancer* 1997; **71**: 355–9.
36 Kondo Y, Kanai Y, Sakamoto M, Mizokami M, Ueda R, Hirohashi S. Genetic instability and aberrant DNA methylation in chronic hepatitis and cirrhosis – a comprehensive study of loss of heterozygosity and microsatellite instability at 39 loci and DNA hypermethylation on 8 CpG islands in microdissected specimens from patients with hepatocellular carcinoma. *Hepatology* 2000; **32**: 970–9.
37 Peng DF, Kanai Y, Sawada M *et al.* DNA methylation of multiple tumor-related genes in association with overexpression of DNA methyltransferase 1 (DNMT1) during multistage carcinogenesis of the pancreas. *Carcinogenesis* 2006; **27**: 1160–8.
38 Kakizoe T. Development and progression of urothelial carcinoma. *Cancer Sci* 2006; **97**: 821–8.
39 Nakagawa T, Kanai Y, Ushijima S, Kitamura T, Kakizoe T, Hirohashi S. DNA hypermethylation on multiple CpG islands associated with increased DNA methyltransferase DNMT1 protein expression during multistage urothelial carcinogenesis. *J Urol* 2005; **173**: 1767–71.
40 Eguchi K, Kanai Y, Kobayashi K, Hirohashi S. DNA hypermethylation at the D17S5 locus in non-small cell lung cancers: its association with smoking history. *Cancer Res* 1997; **57**: 4913–5.
41 Kanai Y, Ushijima S, Ochiai A, Eguchi K, Hui A, Hirohashi S. DNA hypermethylation at the D17S5 locus is associated with gastric carcinogenesis. *Cancer Lett* 1998; **122**: 135–41.
42 Hodge DR, Peng B, Cherry JC *et al.* Interleukin 6 supports the maintenance of p53 tumor suppressor gene promoter methylation. *Cancer Res* 2005; **65**: 4673–82.
43 Kanai Y, Hui AM, Sun L *et al.* DNA hypermethylation at the D17S5 locus and reduced HIC-1 mRNA expression are associated with hepatocarcinogenesis. *Hepatology* 1999; **29**: 703–9.
44 Sawada M, Kanai Y, Arai E, Ushijima S, Ojima H, Hirohashi S. Increased expression of DNA methyltransferase 1 (DNMT1) protein in uterine cervix squamous cell carcinoma and its precursor lesion. *Cancer Lett* 2007; **251**: 211–9.
45 Burgers WA, Blanchon L, Pradhan S, de Launoit Y, Kouzarides T, Fuks F. Viral oncoproteins target the DNA methyltransferases. *Oncogene* 2007; **26**: 1650–5.
46 Kanai Y, Ushijima S, Nakanishi Y, Sakamoto M, Hirohashi S. Mutation of the DNA methyltransferase (DNMT) 1 gene in human colorectal cancers. *Cancer Lett* 2003; **192**: 75–82.
47 Sun L, Hui AM, Kanai Y, Sakamoto M, Hirohashi S. Increased DNA methyltransferase expression is associated with an early stage of human hepatocarcinogenesis. *Jpn J Cancer Res* 1997; **88**: 1165–70.
48 Saito Y, Kanai Y, Sakamoto M, Saito H, Ishii H, Hirohashi S. Expression of mRNA for DNA methyltransferases and methyl-CpG-binding proteins and DNA methylation status on CpG islands and pericentromeric satellite regions during human hepatocarcinogenesis. *Hepatology* 2001; **33**: 561–8.
49 Saito Y, Kanai Y, Nakagawa T *et al.* Increased protein expression of DNA methyltransferase (DNMT) 1 is significantly correlated with the malignant potential and poor prognosis of human hepatocellular carcinomas. *Int J Cancer* 2003; **105**: 527–32.

doi: 10.1111/j.1349-7006.2009.01383.x

50 Peng DF, Kanai Y, Sawada M *et al.* Increased DNA methyltransferase 1 (DNMT1) protein expression in precancerous conditions and ductal carcinomas of the pancreas. *Cancer Sci* 2005; **96**: 403–8.
51 Toyota M, Ahuja N, Ohe-Toyota M, Herman JG, Baylin SB, Issa JP. CpG island methylator phenotype in colorectal cancer. *Proc Natl Acad Sci USA* 1999; **96**: 8681–6.
52 Issa JP. CpG island methylator phenotype in cancer. *Nat Rev Cancer* 2004; **4**: 988–93.
53 Etoh T, Kanai Y, Ushijima S *et al.* Increased DNA methyltransferase 1 (DNMT1) protein expression correlates significantly with poorer tumor differentiation and frequent DNA hypermethylation of multiple CpG islands in gastric cancers. *Am J Pathol* 2004; **164**: 689–99.
54 Kanai Y, Ushijima S, Kondo Y, Nakanishi Y, Hirohashi S. DNA methyltransferase expression and DNA methylation of CPG islands and peri-centromeric satellite regions in human colorectal and stomach cancers. *Int J Cancer* 2001; **91**: 205–12.
55 Ushijima T. Epigenetic field for cancerization. *J Biochem Mol Biol* 2007; **40**: 142–50.
56 Nakagawa T, Kanai Y, Saito Y, Kitamura T, Kakizoe T, Hirohashi S. Increased DNA methyltransferase 1 protein expression in human transitional cell carcinoma of the bladder. *J Urol* 2003; **170**: 2463–6.
57 Wong N, Lam WC, Lai PB, Pang E, Lau WY, Johnson PJ. Hypomethylation of chromosome 1 heterochromatin DNA correlates with q-arm copy gain in human hepatocellular carcinoma. *Am J Pathol* 2001; **159**: 465–71.
58 Nakagawa T, Kanai Y, Ushijima S, Kitamura T, Kakizoe T, Hirohashi S. DNA hypomethylation on pericentromeric satellite regions significantly correlates with loss of heterozygosity on chromosome 9 in urothelial carcinomas. *J Urol* 2005; **173**: 243–6.
59 Hansen RS, Wijmenga C, Luo P *et al.* The DNMT3B DNA methyltransferase gene is mutated in the ICF immunodeficiency syndrome. *Proc Natl Acad Sci USA* 1999; **96**: 14412–7.
60 Saito Y, Kanai Y, Sakamoto M, Saito H, Ishii H, Hirohashi S. Overexpression of a splice variant of DNA methyltransferase 3b, DNMT3b4, associated with DNA hypomethylation on pericentromeric satellite regions during human hepatocarcinogenesis. *Proc Natl Acad Sci USA* 2002; **99**: 10060–5.
61 Soejima K, Fang W, Rollins B. DNA methyltransferase 3b contributes to oncogenic transformation induced by SV40T antigen and activated Ras. *Oncogene* 2003; **22**: 4723–33.
62 Kanai Y, Saito Y, Ushijima S, Hirohashi S. Alterations in gene expression associated with the overexpression of a splice variant of DNA methyltransferase 3b, DNMT3b4, during human hepatocarcinogenesis. *J Cancer Res Clin Oncol* 2004; **130**: 636–44.
63 Estecio MR, Yan PS, Ibrahim AE *et al.* High-throughput methylation profiling by MCA coupled to CpG island microarray. *Genome Res* 2007; **17**: 1529–36.
64 Beck S, Rakyan VK. The methylome: approaches for global DNA methylation profiling. *Trends Genet* 2008; **24**: 231–7.
65 Meissner A, Mikkelsen TS, Gu H *et al.* Genome-scale DNA methylation maps of pluripotent and differentiated cells. *Nature* 2008; **454**: 766–70.
66 Inazawa J, Inoue J, Imoto I. Comparative genomic hybridization (CGH)-arrays pave the way for identification of novel cancer-related genes. *Cancer Sci* 2004; **95**: 559–63.
67 Misawa A, Inoue J, Sugino Y *et al.* Methylation-associated silencing of the nuclear receptor 1I2 gene in advanced-type neuroblastomas, identified by bacterial artificial chromosome array-based methylated CpG island amplification. *Cancer Res* 2005; **65**: 10233–42.
68 Tanaka K, Imoto I, Inoue J *et al.* Frequent methylation-associated silencing of a candidate tumor-suppressor, CRABP1, in esophageal squamous-cell carcinoma. *Oncogene* 2007; **26**: 6456–68.
69 Sugino Y, Misawa A, Inoue J *et al.* Epigenetic silencing of prostaglandin E receptor 2 (PTGER2) is associated with progression of neuroblastomas. *Oncogene* 2007; **26**: 7401–13.
70 Maekita T, Nakazawa K, Mihara M *et al.* High levels of aberrant DNA methylation in Helicobacter pylori-infected gastric mucosae and its possible association with gastric cancer risk. *Clin Cancer Res* 2006; **12**: 989–95.
71 Clark SJ. Action at a distance: epigenetic silencing of large chromosomal regions in carcinogenesis. *Hum Mol Genet* 2007; **16** (Spec No 1): R88–95.
72 Arai E, Ushijima S, Fujimoto H *et al.* Genome-wide DNA methylation profiles in both precancerous conditions and clear cell renal cell carcinomas are correlated with malignant potential and patient outcome. *Carcinogenesis* 2009; **30**: 214–21.
73 Arai E, Kanai Y, Ushijima S, Fujimoto H, Mukai K, Hirohashi S. Regional DNA hypermethylation and DNA methyltransferase (DNMT) 1 protein overexpression in both renal tumors and corresponding nontumorous renal tissues. *Int J Cancer* 2006; **119**: 288–96.
74 Arai E, Ushijima S, Tsuda H *et al.* Genetic clustering of clear cell renal cell carcinoma based on array-comparative genomic hybridization: its association with DNA methylation alteration and patient outcome. *Clin Cancer Res* 2008; **14**: 5531–9.
75 Arai E, Ushijima S, Gotoh M *et al.* Genome-wide DNA methylation profiles in liver tissue at the precancerous stage and in hepatocellular carcinoma. *Int J Cancer* 2009; **125**: 2854–62.
76 Arase Y, Ikeda K, Suzuki F *et al.* Comparison of interferon and lamivudine treatment in Japanese patients with HBeAg positive chronic hepatitis B. *J Med Virol* 2007; **79**: 1286–92.
77 Yoshida H, Tateishi R, Arakawa Y *et al.* Benefit of interferon therapy in hepatocellular carcinoma prevention for individual patients with chronic hepatitis C. *Gut* 2004; **53**: 425–30.
78 Nishiyama N, Arai E, Chihara Y *et al.* Genome-wide DNA methylation profiles in urothelial carcinomas and urothelia at the precancerous stage. *Cancer Sci* 2009; doi: 10.1111/j.1349-7006.2009.01330.x.
79 Mohn F, Schubeler D. Genetics and epigenetics: stability and plasticity during cellular differentiation. *Trends Genet* 2009; **25**: 129–36.

Genome-wide DNA methylation profiles in urothelial carcinomas and urothelia at the precancerous stage

Naotaka Nishiyama,[1,2] Eri Arai,[1] Yoshitomo Chihara,[1] Hiroyuki Fujimoto,[3] Fumie Hosoda,[4] Tatsuhiro Shibata,[4] Tadashi Kondo,[5] Taiji Tsukamoto,[2] Sana Yokoi,[6] Issei Imoto,[6] Johji Inazawa,[6] Setsuo Hirohashi[1] and Yae Kanai[1,7]

[1]Pathology Division, National Cancer Center Research Institute, Tokyo; [2]Urology Division, Sapporo Medical University, Sapporo; [3]Urology Division, National Cancer Center Hospital, Tokyo; [4]Cancer Genomics Project, National Cancer Center Research Institute, Tokyo; [5]Proteome Bioinformatics Project, National Cancer Center Research Institute, Tokyo; [6]Department of Molecular Cytogenetics, Medical Research Institute and School of Biomedical Science, Tokyo Medical and Dental University, Tokyo, Japan

(Received June 16, 2009/Revised August 13, 2009/Accepted August 19, 2009/Online publication September 22, 2009)

To clarify genome-wide DNA methylation profiles during multistage urothelial carcinogenesis, bacterial artificial chromosome (BAC) array-based methylated CpG island amplification (BAMCA) was performed in 18 normal urothelia obtained from patients without urothelial carcinomas (UCs) (C), 17 noncancerous urothelia obtained from patients with UCs (N), and 40 UCs. DNA hypo- and hypermethylation on multiple BAC clones was observed even in N compared to C. Principal component analysis revealed progressive DNA methylation alterations from C to N, and to UCs. DNA methylation profiles in N obtained from patients with invasive UCs were inherited by the invasive UCs themselves, that is DNA methylation alterations in N were correlated with the development of more malignant UCs. The combination of DNA methylation status on 83 BAC clones selected by Wilcoxon test was able to completely discriminate N from C, and diagnose N as having a high risk of carcinogenesis, with 100% sensitivity and specificity. The combination of DNA methylation status on 20 BAC clones selected by Wilcoxon test was able to completely discriminate patients who suffered from recurrence after surgery from patients who did not. The combination of DNA methylation status for 11 BAC clones selected by Wilcoxon test was able to completely discriminate patients with UCs of the renal pelvis or ureter who suffered from intravesical metachronous UC development from patients who did not. Genome-wide alterations of DNA methylation may participate in urothelial carcinogenesis from the precancerous stage to UC, and DNA methylation profiling may provide optimal indicators for carcinogenetic risk estimation and prognostication. (*Cancer Sci* 2010; 101: 231–240)

It is known that DNA hypomethylation results in chromosomal instability as a result of changes in chromatin structure, and that DNA hypermethylation of CpG islands silences tumor-related genes in cooperation with histone modification in human cancers.[1–5] Accumulating evidence suggests that alterations of DNA methylation are involved even in the early and the precancerous stages.[6,7] On the other hand, in patients with cancers, aberrant DNA methylation is significantly associated with poorer tumor differentiation, tumor aggressiveness, and poorer patient outcome.[6,7] Therefore, alterations of DNA methylation may play a significant role in multistage carcinogenesis.

With respect to urothelial carcinogenesis, we have reported accumulation of DNA methylation on C-type CpG islands in a cancer-specific but not age-dependent manner, and protein overexpression of DNA methyltransferase (DNMT) 1, a major DNMT, even in noncancerous urothelia with no apparent histological changes obtained from patients with urothelial carcinomas (UCs).[8,9] Moreover, accumulation of DNA methylation on C-type CpG islands associated with DNMT1 protein overexpression was more frequently evident in aggressive nodular invasive UCs[8–10] resulting in poorer patient outcome than in superficial papillary UCs, which usually remain noninvasive even after repeated urethrocystoscopic resection.[11,12] Since aberrant DNA methylation is one of the earliest molecular events during urothelial carcinogenesis and also participates in tumor aggressiveness, it may be possible to estimate the future risk of developing more malignant UCs. However, only a few previous studies focusing on UCs[13] have employed recently developed array-based technology for assessing genome-wide DNA methylation status,[14–16] and such studies have focused on identification of tumor-related genes that are silenced by DNA methylation.[13] DNA methylation profiles, which could become the optimum indicators for carcinogenetic risk estimation and prognostication of UCs, should therefore be explored using array-based approaches.

In this study, in order to clarify genome-wide DNA methylation profiles during multistage urothelial carcinogenesis, we performed bacterial artificial chromosome (BAC) array-based methylated CpG island amplification (BAMCA)[17–19] using a microarray of 4361 BAC clones[20] in normal urothelia obtained from patients without UCs, noncancerous urothelia obtained from patients with UCs, and UCs themselves.

Materials and Methods

Patients and tissue samples. Seventeen samples of noncancerous urothelia (N1–N17) and 40 samples of UCs (T1–T40) of the urinary bladder, ureter, and renal pelvis were obtained from specimens that had been surgically resected by radical cystectomy (12 patients) or nephroureterectomy (28 patients) at the National Cancer Center Hospital, Tokyo, Japan. The patients comprised 31 men and nine women whose mean age was 69.03 ± 9.77 (mean ± SD) years (range, 49–85 years). Microscopic examination revealed no remarkable histological changes in the noncancerous urothelia. The patients from whom noncancerous urothelia were obtained comprised 11 men and six women with a mean age of 70.41 ± 9.33 (mean ± SD) years (range, 49–85 years). There were 17 superficial UCs (two pTa and 15 pT1 tumors) and 23 invasive UCs (six pT2, 16 pT3, and one pT4 tumor) according to the criteria proposed by World Health Organization classification.[21] For comparison, 18 samples of normal urothelia obtained from patients without UCs (C1–C18) were used. Fourteen, three, and one patient underwent nephrectomy for renal cell carcinoma, nephrectomy for retroperitoneal sarcoma around the kidney, and partial cystectomy for urachal carcinoma, respectively. The patients from whom normal urothelia were obtained comprised 13 men and five women with a mean age of 61.17 ± 15.16 (mean ± SD) years (range, 27–82 years). This study was approved by the Ethics Committee of the National Cancer Center, Tokyo, Japan and has

[7]To whom correspondence should be addressed. E-mail: ykanai@ncc.go.jp

doi: 10.1111/j.1349-7006.2009.01330.x

been performed in accordance with the Declaration of Helsinki in 1995. All patients gave their informed consent prior to their inclusion in this study.

BAMCA. High-molecular-weight DNA from fresh frozen tissue samples was extracted using phenol-chloroform, followed by dialysis. Because DNA methylation status is known to be organ-specific,[22] the reference DNA for analysis of the developmental stages of UCs should be obtained from the urothelium, and not from other organs or peripheral blood. Therefore, a mixture of normal urothelial DNA obtained from 11 male patients (C19–C29) and six female patients (C30–C35) without UCs was used as a reference for analyses of male and female test DNA samples, respectively. DNA methylation status was analyzed by BAMCA using a custom-made array (MCG Whole Genome Array-4500) harboring 4361 BAC clones located throughout chromosomes 1–22, X and Y,[20] as described previously.[17–19] Briefly, 5-μg aliquots of test or reference DNA were first digested with 100 units of the methylation-sensitive restriction enzyme Sma I and subsequently with 20 units of the methylation-insensitive Xma I. Adapters were ligated to the Xma I-digested sticky ends, and PCR was performed with an adapter primer set. Test and reference PCR products were labeled by random priming with Cy3- and Cy5-dCTP (GE Healthcare, Buckinghamshire, UK), respectively, and precipitated together with ethanol in the presence of Cot-I DNA. The mixture was applied to array slides and incubated at 43°C for 72 h. Arrays were scanned with a GenePix Personal 4100A (Axon Instruments, Foster City, CA, USA) and analyzed using GenePix Pro 5.0 imaging software (Axon Instruments) and Acue 2 software (Mitsui Knowledge Industry, Tokyo, Japan). The signal ratios were normalized in each sample to make the mean signal ratios of all BAC clones 1.0.

Statistics. Differences in the average number of BAC clones that showed DNA methylation alterations (DNA hypo- and hypermethylation) between groups of samples were analyzed using the Mann–Whitney *U*-test. Differences at $P < 0.05$ were considered significant. Principal component analysis based on BAMCA data was performed using the Expressionist software program (Gene Data, Basel, Switzerland). Unsupervised two-dimensional hierarchical clustering analysis of tissue samples and the BAC clones were performed using the Expressionist software program. Correlations between the subclassification of patients yielded by unsupervised hierarchical clustering analysis and clinicopathological parameters of UCs were analyzed using the χ^2-test. Differences at $P < 0.05$ were considered significant. BAC clones whose signal ratios yielded by BAMCA were significantly different between groups of samples were identified by Wilcoxon test ($P < 0.01$).

Results

Genome-wide DNA methylation alterations during multistage urothelial carcinogenesis. Figure 1(b,c) shows examples of scanned array images and scattergrams of the signal ratios (test signal/reference signal), respectively, for normal urothelium from a patient without UC (panel C), and both noncancerous urothelium (panel N) and cancerous tissue (panel T) from a patient with UC. In all normal urothelia (C1–C18), the signal ratios of 97% of the BAC clones were between 0.67 and 1.5 (red bars in Fig. 1c). Therefore, in noncancerous urothelia obtained from patients with UCs and UCs, DNA methylation status corresponding to a signal ratio of less than 0.67 and more than 1.5 was defined as DNA hypomethylation and DNA hypermethylation of each BAC clone compared to normal urothelia, respectively, as in our previous study.[23] In noncancerous urothelia obtained from patients with UCs, many BAC clones showed DNA hypo- or hypermethylation (panel N of Fig. 1c). In UCs themselves, more BAC clones showed DNA hypo- or hypermethylation, and the degree of DNA hypo- or hypermethylation, that is deviation of the signal ratio from 0.67 or 1.5, was increased (panel T of Fig. 1c) in comparison with noncancerous urothelia obtained from patients with UCs. The average number of BAC clones showing DNA hypomethylation increased significantly from noncancerous urothelia obtained from patients with UCs (24.53 ± 31.48) to UCs (236.78 ± 92.78, $P = 4.37e\text{-}9$). The average number of BAC clones showing DNA hypermethylation increased significantly from noncancerous urothelia obtained from patients with UCs (29.18 ± 39.84) to UCs (289.13 ± 82.42, $P = 7.35e\text{-}9$). Principal component analysis based on BAMCA data (signal ratios) revealed progressive DNA methylation alterations from normal urothelia, to noncancerous urothelia obtained from patients with UCs, and to UCs (Fig. 1d).

Clinicopathological significance of DNA methylation alterations in noncancerous urothelia obtained from patients with UCs. In order to clarify the clinicopathological significance of DNA methylation alterations in noncancerous urothelia obtained from patients with UCs, unsupervised two-dimensional hierarchical clustering analysis based on BAMCA data (signal ratios) for noncancerous urothelia was performed. Seventeen patients with UCs were clustered into two subclasses, Clusters A_N and B_N, which contained nine and eight patients, respectively, based on the DNA methylation status of the noncancerous urothelia (Fig. 2a). All eight patients (100%) belonging to Cluster B_N suffered from invasive UCs (pT2 or more), whereas five (55.6%) of the patients belonging to Cluster A_N did so ($P = 0.0311$).

The Wilcoxon test ($P < 0.01$) revealed that the signal ratios of 131 BAC clones differed significantly between noncancerous urothelia obtained from patients with superficial UCs (pTa and pT1) and noncancerous urothelia obtained from patients with invasive UCs (pT2 or more). If the average signal ratios in noncancerous urothelia obtained from patients with invasive UCs were significantly higher than those in noncancerous urothelia obtained from patients with superficial UCs (67 BAC clones), the average signal ratios in the invasive UCs themselves were even higher than (42 BAC clones, e.g. RP11-79K14 and RP11-29C11 in Fig. 2b) or not significantly different from (25 BAC clones, e.g. RP11-3A9 and RP11-73G16 in Fig. 2b) those in noncancerous urothelia obtained from patients with invasive UCs, without exception. If the average signal ratios in noncancerous urothelia obtained from patients with invasive UCs were significantly lower than those in noncancerous urothelia obtained from patients with superficial UCs (64 BAC clones), the average signal ratios in the invasive UCs themselves were even lower than (38 BAC clones, e.g. RP11-210F15 and RP11-368O13 in Fig. 2b) or not significantly different from (26 BAC clones, e.g. RP11-442N24 and RP11-65C22 in Fig. 2b) those in noncancerous urothelia obtained from patients with invasive UCs, without exception, that is DNA methylation status of the 131 BAC clones in noncancerous urothelia obtained from patients with invasive UCs was inherited by the invasive UCs themselves.

DNA methylation profiles discriminating noncancerous urothelia obtained from patients with UCs from normal urothelia. Our finding that DNA methylation alterations in noncancerous urothelia were correlated with the development of UCs, as described above, prompted us to estimate the degree of carcinogenetic risk based on DNA methylation profiles in noncancerous urothelia. We attempted to establish criteria for indicating that noncancerous urothelia obtained from patients with UCs, and not normal urothelia, were at high risk of carcinogenesis.

The Wilcoxon test ($P < 0.01$) revealed that the signal ratios on 201 BAC clones differed significantly between normal urothelia obtained from patients without UCs and noncancerous urothelia obtained from patients with UCs. Figure 3(a) shows

doi: 10.1111/j.1349-7006.2009.01330.x

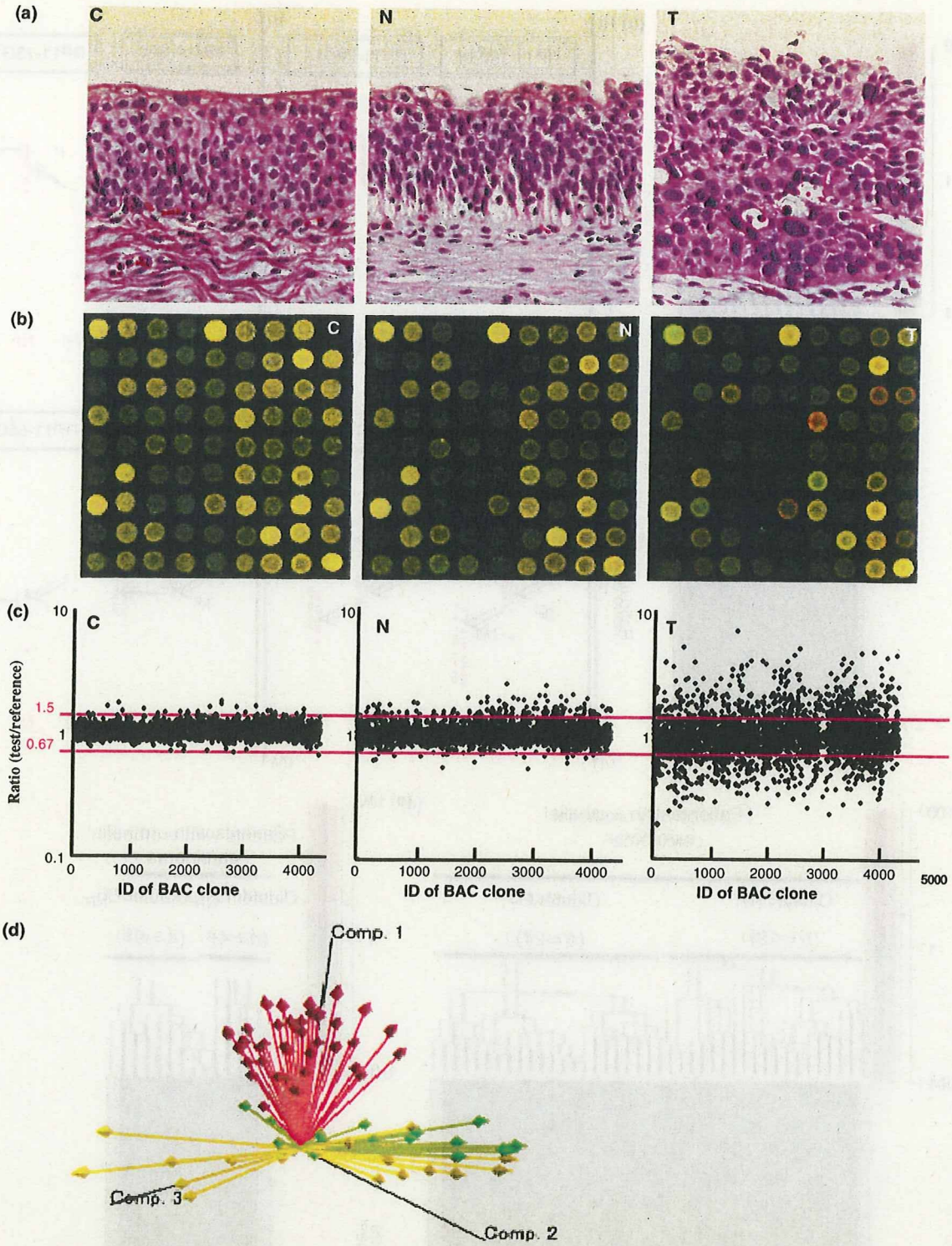

Fig. 1. DNA methylation alterations during multistage urothelial carcinogenesis. (a) Microscopic view of normal urothelium obtained from a patient without urothelial carcinoma (UC) (C), noncancerous urothelium obtained from a patient with UC (N), and UC (T). N shows no remarkable histological changes in comparison to C, that is no cytological or structural atypia is evident. Hematoxylin–eosin staining. Original magnification, ×20. (b) Scanned array images obtained by bacterial artificial chromosome (BAC) array-based methylated CpG island amplification (BAMCA) in C, N, and T. Co-hybridization was done with test and reference DNA labeled with Cy3 and Cy5, respectively. (c) Scattergrams of the signal ratios (test signal/reference signal) obtained by BAMCA in C, N, and T. In all 18 normal urothelia (C1–C18), the signal ratios of 97% of the BAC clones were between 0.67 and 1.5 (red bars). Therefore, in N and T, DNA methylation status corresponding to a signal ratio of less than 0.67 and more than 1.5 was defined as DNA hypomethylation and DNA hypermethylation on each BAC clone compared to C, respectively. Even though N did not show any marked histological changes in comparison to C (panels C and N in [a]), many BAC clones showed DNA hypo- or hypermethylation. In T, more BAC clones showed DNA hypo- or hypermethylation, whose degree, that is deviation of the signal ratio from 0.67 or 1.5, was increased in comparison to N. (d) Principal component analysis based on BAMCA data (signal ratios). Progressive alterations of DNA methylation status from normal urothelia (yellow arrows) to noncancerous urothelia obtained from patients with UCs (green arrows), and to UCs (red arrows) were observed.

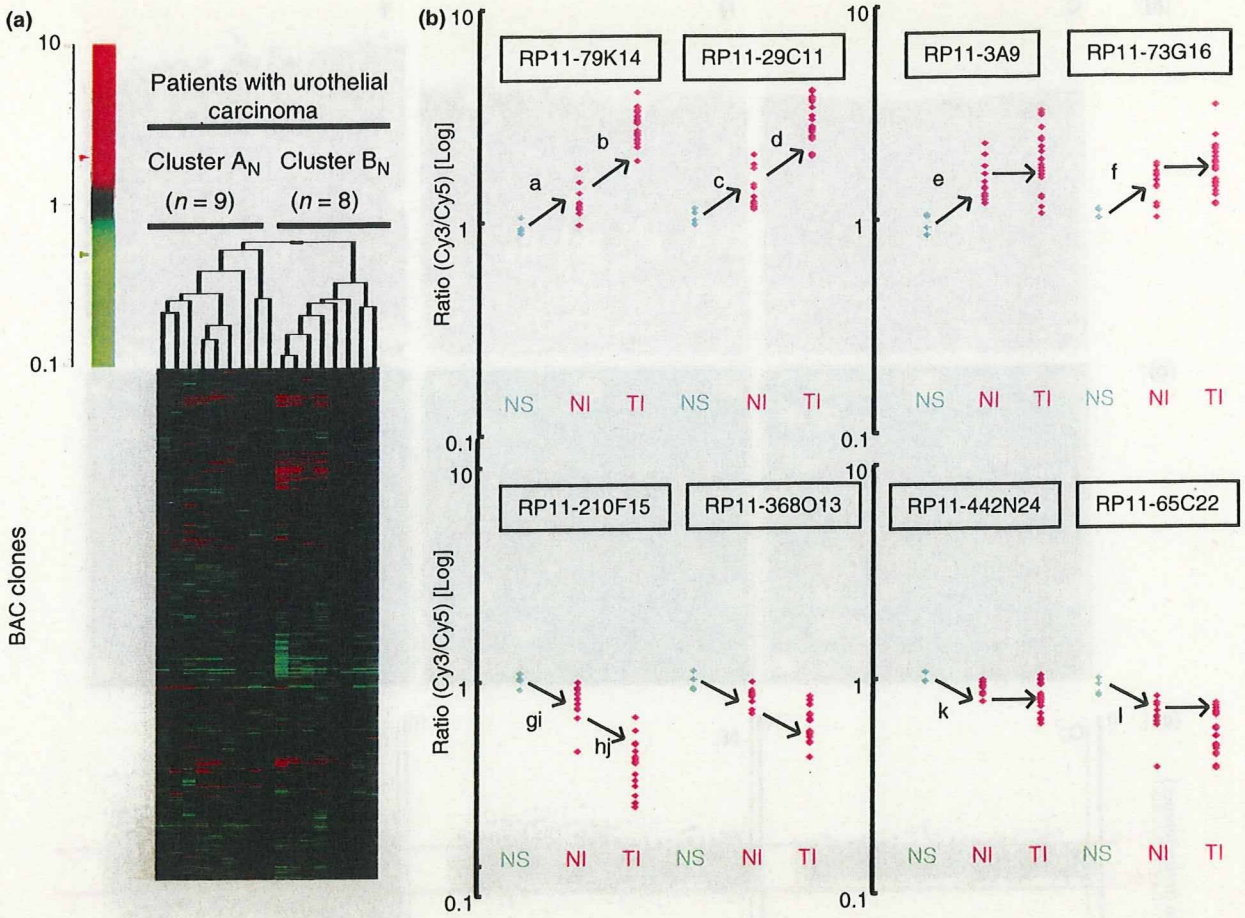

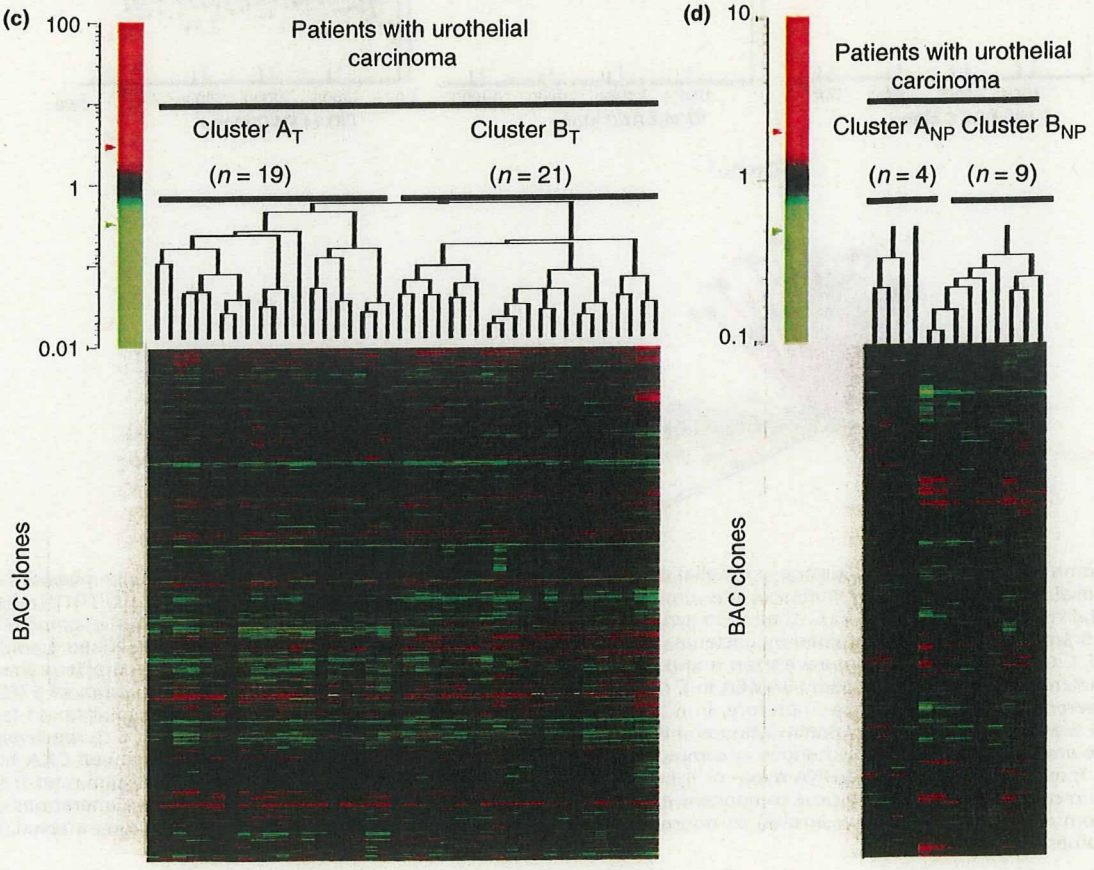

doi: 10.1111/j.1349-7006.2009.01330.x

Fig. 2. Correlations between DNA methylation status and clinicopathological parameters. (a) Unsupervised two-dimensional hierarchical clustering analysis based on bacterial artificial chromosome (BAC) array-based methylated CpG island amplification (BAMCA) data (signal ratios) in noncancerous urothelia obtained from patients with urothelial carcinomas (UCs). The signal ratio is shown in the color range map. Seventeen patients with UCs were hierarchically clustered into two subclasses, Clusters A_N (n = 9) and B_N (n = 8). Eight patients (100%) belonging to Cluster B_N developed invasive UCs (pT2 or more), whereas five patients (55.6%) belonging to Cluster A_N did so (P = 0.0311). (b) Scattergrams of the signal ratios in tissue samples. NS, noncancerous urothelia obtained from patients with superficial UCs. NI, noncancerous urothelia obtained from patients with invasive UCs. TI, invasive UCs. If the average signal ratios in NI were significantly higher than those in NS, the average signal ratios in TI themselves were even higher than (BAC clones RP11-79K14 and RP11-29C11), or not significantly different from (BAC clones RP11-3A9 and RP11-73G16), those in NI without exception. If the average signal ratios in NI were significantly lower than those in NS, the average signal ratios in TI themselves were even lower than (BAC clones RP11-210F15 and RP11-368O13), or not significantly different from (BAC clones RP11-442N24 and RP11-65C22), those in NI without exception. ^{a}P = 0.001680673, ^{b}P = 9.23504e-7, ^{c}P = 0.002197802, ^{d}P = 3.64223e-6, ^{e}P = 0.000840336, ^{f}P = 0.007692306, ^{g}P = 0.004395604, ^{h}P = 8.31509e-6, ^{i}P = 0.004395604, ^{j}P = 1.10173e-5, ^{k}P = 0.005882353, ^{l}P = 0.001098901. (c) Unsupervised two-dimensional hierarchical clustering analysis based on BAMCA data (signal ratios) in UCs. Forty patients with UCs were hierarchically clustered into two subclasses, Clusters A_T (n = 19) and B_T (n = 21). All four patients with recurrence belonged to Cluster B_T. (d) Unsupervised two-dimensional hierarchical clustering analysis based on BAMCA data (signal ratios) for noncancerous urothelia obtained from patients with UCs of the renal pelvis or ureter. Thirteen patients with UCs of the renal pelvis or ureter were hierarchically clustered into two subclasses, Clusters A_{NP} (n = 4) and B_{NP} (n = 9). All four patients who developed intravesical metachronous UC belonged to Cluster B_{NP}.

scattergrams of the signal ratios in normal urothelia and noncancerous urothelia obtained from patients with UCs for representative examples of the 201 BAC clones. Using the cut-off values described in Figure 3(a), noncancerous urothelia obtained from patients with UCs were discriminated from normal urothelia with sufficient sensitivity and specificity (Fig. 3a). From the 201 BAC clones, 83 for which such discrimination was performed with a sensitivity and specificity of 75% or more than 75% were selected (Table S1). The cut-off values of the signal ratios for the 83 BAC clones, and their sensitivity and specificity, are shown in Table S1.

A histogram showing the number of BAC clones satisfying the criteria listed in Table S1 for 18 normal urothelia (C1–C18) and 17 noncancerous urothelia obtained from patients

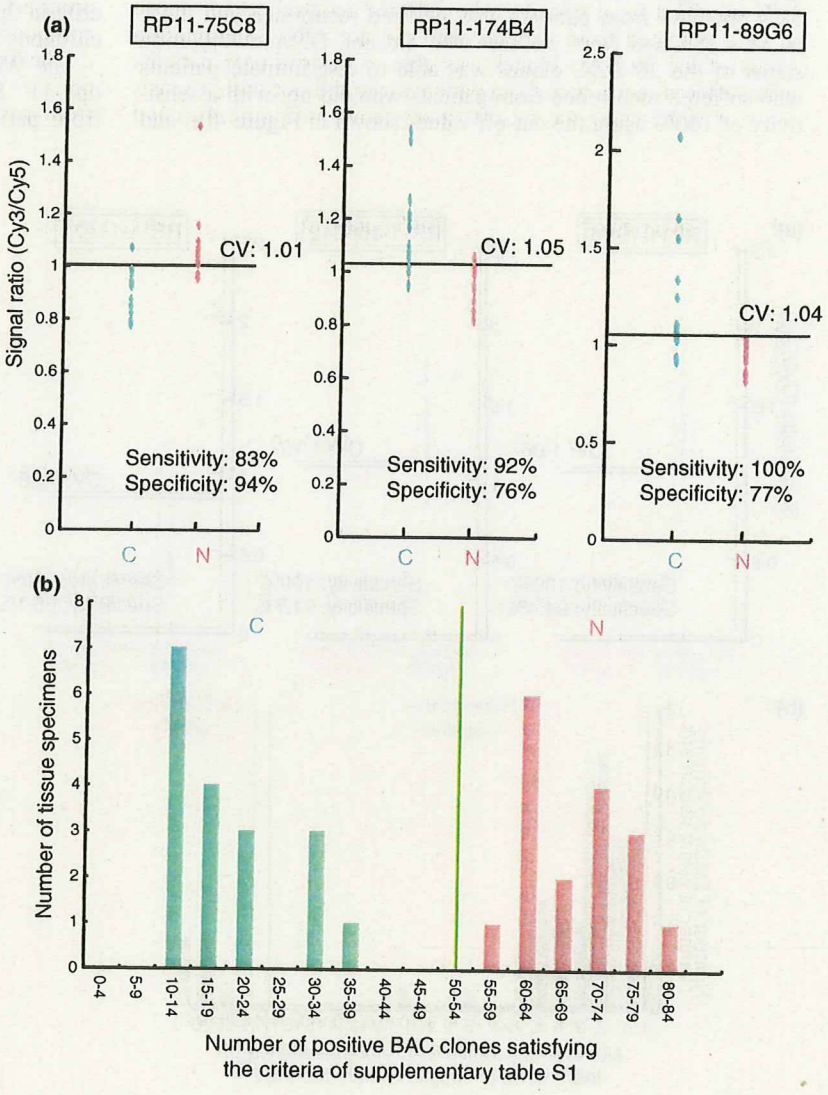

Fig. 3. DNA methylation profiles discriminating noncancerous urothelia obtained from patients with urothelial carcinomas (UCs) (N) from normal urothelia (C). (a) Scattergrams of the signal ratios in C and N on representative bacterial artificial chromosome (BAC) clones, RP11-75C8, RP11-174B4, and RP11-89G6. Using the cut-off values (CV) described in each panel, N in this cohort were discriminated from C with sufficient sensitivity and specificity. (b) Histogram showing the number of BAC clones satisfying the criteria listed in Table S1 in samples C1–C18 and N1–N17. Based on this histogram, we established a criterion that when the noncancerous urothelia satisfied the criteria in Table S1 for 50 (green bar) or more than 50 BAC clones, they were judged to be at high risk of carcinogenesis.

with UCs (N1–N17) is shown in Figure 3(b). Based on this figure, we finally established the following criteria: when noncancerous urothelia satisfied the criteria in Table S1 for 50 or more BAC clones (green bar in Fig. 3b), they were judged to be at high risk of carcinogenesis, and when noncancerous urothelia satisfied the criteria in Table S1 for less than 50 BAC clones, they were judged not to be at high risk of carcinogenesis. Based on these criteria, both the sensitivity and specificity for diagnosis of noncancerous urothelia obtained from patients with UCs in this cohort as being at high risk of carcinogenesis were 100%.

Association of DNA methylation profiles in UCs with recurrence. Unsupervised two-dimensional hierarchical clustering analysis based on BAMCA data (signal ratios) for UCs was able to group 40 patients into two subclasses, Clusters A_T and B_T, which contained 19 and 21 patients, respectively (Fig. 2c). Four patients (19.0%) belonging to Cluster B_T suffered recurrence after surgery (metastasis to the pelvic lymph nodes in three, and metastasis to the lung and bone in one), whereas none (0%) belonging to Cluster A_T did so ($P = 0.0449$). The mean observation period was 29.8 ± 28.0 months (mean ± SD). These data prompted us to establish criteria for predicting recurrence of UCs based on DNA methylation status.

The Wilcoxon test ($P < 0.01$) revealed that the signal ratios on 20 BAC clones in UCs differed significantly between the patients who suffered recurrence after surgery and patients who did not. Figure 4(a) shows scattergrams of the signal ratios in UCs obtained from patients who suffered recurrence and those in UCs obtained from patients who did not. DNA methylation status of the 20 BAC clones was able to discriminate patients who suffered recurrence from patients who did not with a sensitivity of 100% using the cut-off values shown in Figure 4(a) and Table S2. A histogram showing the number of BAC clones satisfying the criteria listed in Table S2 for all 40 UCs is shown in Figure 4(b). Satisfying the criteria in Table S2 for 17 or more BAC clones (green bar in Fig. 4b) discriminated patients who suffered recurrence from patients who did not with a sensitivity and specificity of 100%, whereas high histological grade,[21] invasive growth (pT2 or more), and vascular or lymphatic involvement were unable to achieve such complete discrimination (data not shown).

Association of DNA methylation profiles in noncancerous urothelia obtained from patients with UCs of the renal pelvis or ureter with intravesical metachronous UC development. It is well known that patients with UCs of the renal pelvis and ureter frequently suffer from metachronous UC development in the urinary bladder after nephroureterectomy.[24,25] Since such metachronous UC originates from the noncancerous urothelium of the urinary bladder, we focused on the DNA methylation status of noncancerous urothelia obtained by nephroureterectomy from patients with UCs of the renal pelvis or ureter. Unsupervised two-dimensional hierarchical clustering analysis based on BAMCA data (signal ratios) for noncancerous urothelia obtained from patients with UCs of the renal pelvis or ureter was able to group 13 patients into two subclasses, Clusters A_{NP} and B_{NP}, which contained four and nine patients, respectively (Fig. 2d). Four (44%) of the patients in Cluster B_{NP} developed intravesical metachronous UCs, whereas none (0%) belonging to Cluster A_{NP} did so. These data prompted us to establish criteria that could predict the development of intravesical metachronous UC based on DNA methylation status.

The Wilcoxon test ($P < 0.01$) revealed that the signal ratios on 11 BAC clones in noncancerous urothelia obtained from patients with UCs of the renal pelvis or ureter differed

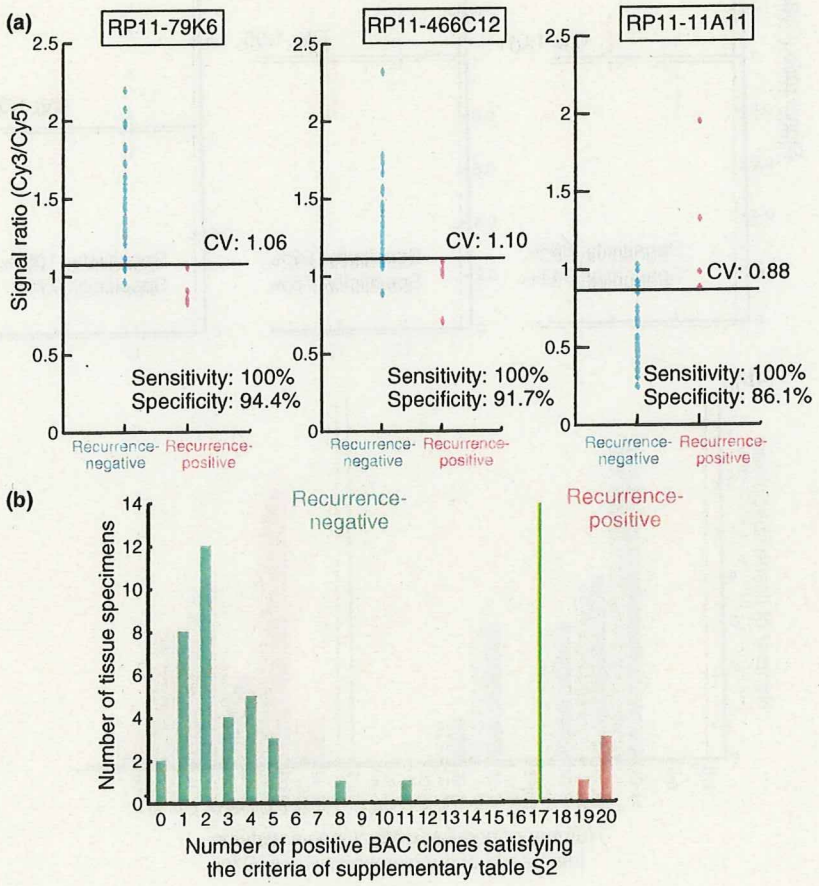

Fig. 4. DNA methylation profiles in urothelial carcinomas (UCs) associated with recurrence. (a) Scattergrams of the signal ratios in UCs from patients who did not develop recurrence ($n = 36$) and UCs from patients who developed recurrence ($n = 4$) on representative bacterial artificial chromosome (BAC), clones, RP11-79K6, RP11-466C12, and RP11-11A11. Using the cut-off values (CV) described in each panel, recurrence-positive patients were discriminated from recurrence-negative patients with 100% sensitivity. (b) Histogram showing the number of BAC clones satisfying the criteria listed in Table S2 in all 40 patients with UCs. Satisfying the criteria in Table S2 for 17 (green bar) or more than 17 BAC clones discriminated recurrence-positive patients from recurrence-negative patients with a sensitivity and specificity of 100%, whereas high histological grade (21), invasive growth (pT2 or more), and vascular or lymphatic involvement were unable to achieve such complete discrimination (data not shown).

doi: 10.1111/j.1349-7006.2009.01330.x

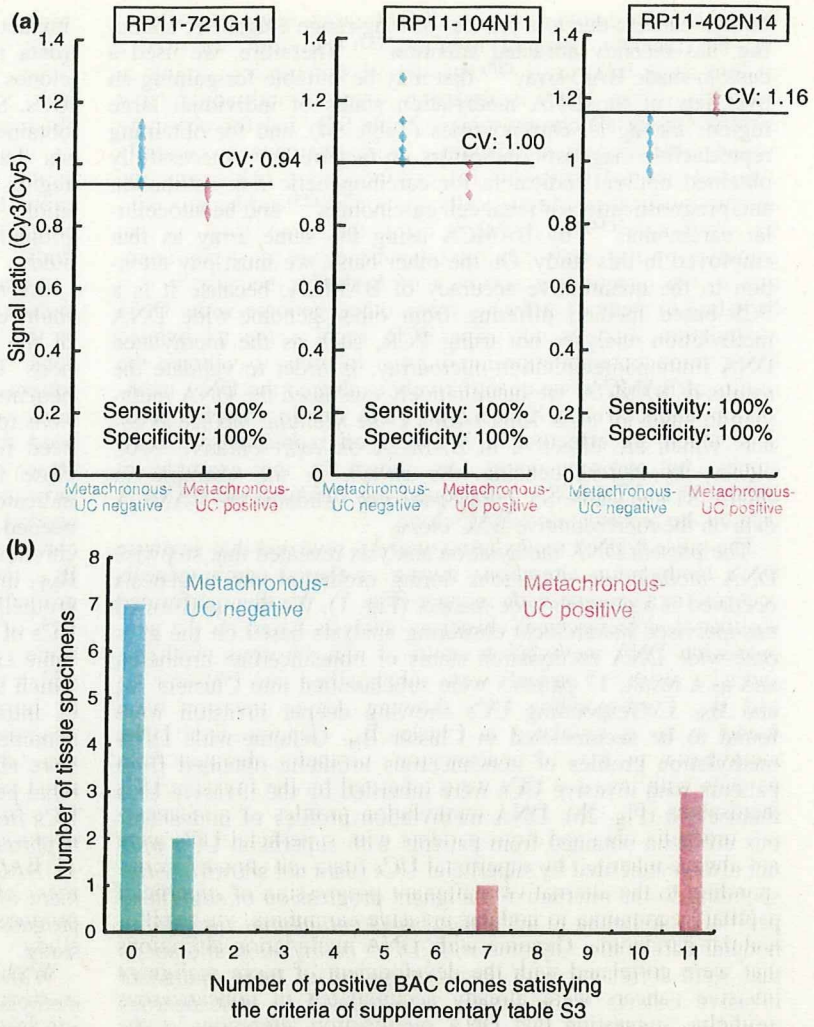

Fig. 5. DNA methylation profiles in noncancerous urothelia obtained from patients with urothelial carcinomas (UCs) of the renal pelvis or ureter associated with intravesical metachronous UC development. (a) Scattergrams of the signal ratios in noncancerous urothelia obtained from patients who did not develop intravesical metachronous UCs ($n = 9$) and noncancerous urothelia obtained from patients who developed intravesical metachronous UCs ($n = 4$) on representative bacterial artificial chromosome (BAC) clones, RP11-721G11, RP11-104N11, and RP11-402N14. Using the cut-off values (CV) described in each panel, metachronous UC-positive patients were discriminated from metachronous UC-negative patients with 100% sensitivity and specificity. (b) Histogram showing the number of BAC clones satisfying the criteria listed in Table S3 in all 13 patients with UCs of the renal pelvis or ureter from whom noncancerous urothelia were obtained. Patients who were negative and positive for metachronous UC were confirmed to show a marked difference in the DNA methylation status of the 11 BAC clones.

significantly between patients who developed intravesical metachronous UC after nephroureterectomy and patients who did not. DNA methylation status of nine of the 11 BAC clones was able to discriminate patients who suffered from intravesical metachronous UC development from patients who did not with a sensitivity and specificity of 100% using the cut-off values shown in Figure 5(a) and Table S3. A histogram showing the number of BAC clones satisfying the criteria listed in Table S3 for 13 noncancerous urothelia obtained from patients with UCs of the renal pelvis or ureter is shown in Figure 5(b).

Discussion

Urothelial carcinomas are clinically remarkable because of their multicentricity: synchronously or metachronously multifocal UCs often develop in individual patients. A possible mechanism for such multiplicity is the "field effect," whereby carcinogenic agents in the urine cause malignant transformation of multiple urothelial cells.[26] Even noncancerous urothelia showing no remarkable histological features obtained from patients with UCs can be considered to be at the precancerous stage, because they may be exposed to carcinogens in the urine. On the other hand, UCs are classified as superficial papillary carcinomas or nodular invasive carcinomas according to their configuration. Superficial papillary carcinomas usually remain noninvasive, although patients need to undergo repeated urethrocystoscopic resections because of recurrences. In contrast, the clinical outcome of nodular invasive carcinomas is poor.[11,12]

In our previous study, accumulation of DNA methylation on C-type CpG islands associated with DNMT1 protein overexpression was observed even in noncancerous urothelia obtained from patients with UCs.[8,9] Aberrant DNA methylation was further increased, especially in nodular invasive carcinomas.[8–10] These previous data suggested that carcinogenetic risk estimation and prognostication of UCs based on DNA methylation status might be a promising strategy. Although optimal diagnostic indicators have never been explored using array-based genome-wide DNA methylation analysis, alterations of DNA methylation on several CpG islands in UCs have been reported separately.[27–31]

Many researchers in the field of cancer epigenetics have used promoter arrays to identify the genes that are methylated in cancer cells.[14–16] However, the promoter regions of specific genes are not the only target of DNA methylation alterations in human cancers. DNA methylation status in genomic regions that do not directly participate in gene silencing, such as the edges of CpG islands, may be altered at the precancerous stage before the alterations of the promoter regions themselves occur.[32] Genomic regions in which DNA hypomethylation affects chromosomal instability may not be contained in promoter arrays. Moreover, aberrant DNA methylation of large regions of chromosomes, which are regulated in a coordinated manner in

human cancers due to a process of long-range epigenetic silencing, has recently attracted attention.[33] Therefore, we used a custom-made BAC array[20] that may be suitable for gaining an overview of the DNA methylation status of individual large regions among all chromosomes (Table S4), and for obtaining reproducible diagnostic indicators. In fact we have successfully obtained optimal indicators for carcinogenetic risk estimation and prognostication of renal cell carcinomas[23] and hepatocellular carcinomas[34] by BAMCA using the same array as that employed in this study. On the other hand, we must pay attention to the quantitative accuracy of BAMCA, because it is a PCR-based method differing from other genome-wide DNA methylation analyses not using PCR, such as the methylated DNA immunoprecipitation-microarray. In order to validate the results of BAMCA, we quantitatively evaluated the DNA methylation status of each Xma I/Sma I site yielding labeled products which are effective in BAMCA on representative BAC clones, by pyrosequencing. As shown in the example in Figure S1 and Table S5, pyrosequencing validated the BAMCA data on the representative BAC clone.

The present DNA methylation analysis revealed that stepwise DNA methylation alterations during urothelial carcinogenesis occurred in a genome-wide manner (Fig. 1). We then performed unsupervised hierarchical clustering analysis based on the genome-wide DNA methylation status of noncancerous urothelia, and as a result, 17 patients were subclassified into Clusters A_N and B_N. Corresponding UCs showing deeper invasion were found to be accumulated in Cluster B_N. Genome-wide DNA methylation profiles of noncancerous urothelia obtained from patients with invasive UCs were inherited by the invasive UCs themselves (Fig. 2b). DNA methylation profiles of noncancerous urothelia obtained from patients with superficial UCs were not always inherited by superficial UCs (data not shown), corresponding to the alternative malignant progression of superficial papillary carcinoma to nodular invasive carcinoma, via papillonodular carcinoma. Genome-wide DNA methylation alterations that were correlated with the development of more malignant invasive cancers were already accumulated in noncancerous urothelia, suggesting that DNA methylation alterations at the precancerous stage may not occur randomly but are prone to further accumulation of genetic and epigenetic alterations and generate more malignant cancers.

The present genome-wide analysis revealed DNA methylation profiles that were able to completely discriminate noncancerous urothelia obtained from patients with UCs from normal urothelia and diagnose them as having a high risk of urothelial carcinogenesis with a sensitivity and specificity of 100%. We are currently attempting to develop methodology for assessing the tendency for DNA methylation in the 83 BAC regions in urine samples with a view to application for screening of healthy individuals. If it proves possible to identify individuals who are at high risk of urothelial carcinogenesis, then strategies for the prevention or early detection of UCs, such as smoking cessation or repeated urine cytology examinations, might be applicable.

Even after surgery with curative intent, some UCs relapse and metastasize to lymph nodes or distant organs.[35] Recently, new systemic chemotherapy and targeted therapy have been developed for treatment for UCs.[36] In order to start adjuvant systemic chemotherapy immediately in patients who have undergone surgery and are still at high risk of recurrence and metastasis, prognostic indicators have been explored. The present genome-wide analysis revealed DNA methylation profiles that were able to discriminate patients who suffered recurrence after surgery from patients who did not with a sensitivity and specificity of 100% (Fig. 4b), whereas a high histological grade,[21] invasive growth (pT2 or more), and vascular or lymphatic involvement, which are known to have a prognostic impact,[37,38] were incapable of such complete discrimination (data not shown). Therefore, a combination of the 20 BAC clones can have significant prognostic value for patients with UCs. Since a sufficient quantity of good-quality DNA can be obtained from each surgical specimen, our array-based analysis that overviews aberrant DNA methylation of each BAC region is immediately applicable to routine laboratory examinations for prognostication after surgery. The reliability of such prognostication will need to be validated in a prospective study.

As mentioned above, UCs are remarkable because of their multicentricity. Approximately 10–30% of patients with UCs of the renal pelvis and ureter develop intravesical metachronous UCs after nephroureterectomy.[24,25] Therefore, such patients have to undergo repeated urethrocystoscopic examinations to detect intravesical metachronous UCs. To decrease the need for invasive urethrocystoscopic examinations and assist close follow-up of such patients after nephroureterectomy, indicators for intravesical metachronous UCs have been needed. All of our patients who developed intravesical metachronous UCs after nephroureterectomy belonged to Cluster B_{NP}, indicating that DNA methylation profiles of noncancerous urothelia obtained by nephroureterectomy from patients with UCs of the renal pelvis or ureter, which may be exposed to the same carcinogens in the urine as noncancerous urothelia from which metachronous UCs originate, are correlated with the risk of intravesical metachronous UC development. The present genome-wide analysis revealed DNA methylation profiles that were able to completely discriminate patients with UCs of the renal pelvis or ureter who developed intravesical metachronous UCs from patients who did not, in noncancerous urothelia from nephroureterectomy specimens. A combination of the present 11 BAC clones may be an optimal indicator for the development of intravesical metachronous UC. The reliability of such prognostication will again need to be validated in a prospective study.

With respect to background factors of genome-wide DNA methylation alterations during urothelial carcinogenesis, smoking history did not correlate significantly with the numbers of BAC clones showing DNA hypo- or hypermethylation in noncancerous urothelia obtained from patients with UCs and in UCs, or with clustering (Cluster A_N *vs* Cluster B_N and Cluster A_T *vs* Cluster B_T) (Table S6). In addition, immunohistochemically examined DNMT1 protein expression levels did not correlate significantly with the numbers of BAC clones showing DNA hypo- or hypermethylation in noncancerous urothelia obtained from patients with UCs and in UCs, or with clustering (Cluster A_N *vs* Cluster B_N and Cluster A_T *vs* Cluster B_T) (Table S7), indicating that expression levels of DNMT1 did not by themselves simply determine DNA methylation profiles. However, our previous study revealed remarkable protein overexpression of DNMT1 in noncancerous urothelia obtained from patients with UCs as compared to normal urothelia.[8] Therefore, undefined cofactors may recruit DNMT1 or other proteins regulating DNA methylation status to aberrant target sequences and may participate in DNA methylation alterations in noncancerous urothelia obtained from patients with UCs. Further studies are needed to elucidate molecular mechanisms of DNA methylation alterations in such noncancerous urothelia.

Moreover, when the DNA methylation status for CpG islands of *p16*, human MutL homologue 1 (*hMLH1*), thrombospondin-1 (*THBS-1*), and death-associated protein kinase (*DAPK*) genes and the methylated in tumor (MINT)-1, -2, -12, -25, and -31 clones were examined in noncancerous urothelia obtained from patients with UCs and in UCs by methylation-specific PCR and combined bisulfite restriction enzyme analysis as in our previous study,[9,39] the incidence of DNA

doi: 10.1111/j.1349-7006.2009.01330.x

methylation on each CpG island and the average number of methylated CpG islands did not correlate significantly with the numbers of BAC clones showing DNA hypo- or hypermethylation in noncancerous urothelia obtained from patients with UCs and in UCs, or with clustering (Cluster A_N *vs* Cluster B_N and Cluster A_T *vs* Cluster B_T) (Table S8). Therefore, molecular mechanisms for alterations of genome-wide DNA methylation profiles may differ from those for regional DNA hypermethylation on CpG islands.

Although BAMCA mainly provides an overview of the DNA methylation status of individual large regions among all chromosomes as mentioned above, it may also be able to identify genes for which expressions are regulated by DNA methylation, since there are promoter regions of specific genes including CpG islands on BAC clones showing clinicopathologically significant DNA hypo- or hypermethylation (Table S4). Expression levels and the DNA methylation status of these genes, as well as the functions of the proteins coded by such genes, will be examined in a future investigation. If further studies identify tumor-related genes for which expression levels are regulated by DNA methylation among such candidates, these tumor-related genes may serves as targets for epigenetic prevention and therapy, along with the molecules causing alterations of genome-wide DNA methylation profiles.

Acknowledgments

This study was supported by a Grant-in-Aid for the Third Term Comprehensive 10-Year Strategy for Cancer Control from the Ministry of Health, Labor and Welfare of Japan; a Grant-in-Aid for Cancer Research from the Ministry of Health, Labor and Welfare of Japan; a Grant from the New Energy and Industrial Technology Development Organization (NEDO); and the Program for Promotion of Fundamental Studies in Health Sciences of the National Institute of Biomedical Innovation (NiBio). N. Nishiyama is an awardee of a research resident fellowship from the Foundation for Promotion of Cancer Research in Japan.

References

1 Jones PA, Baylin SB. The fundamental role of epigenetic events in cancer. *Nat Rev Genet* 2002; **3**: 415–28.
2 Eden A, Gaudet F, Waghmare A, Jaenisch R. Chromosomal instability and tumors promoted by DNA hypomethylation. *Science* 2003; **300**: 455.
3 Baylin SB, Ohm JE. Epigenetic gene silencing in cancer – a mechanism for early oncogenic pathway addiction? *Nat Rev Cancer* 2006; **6**: 107–16.
4 Gronbaek K, Hother C, Jones PA. Epigenetic changes in cancer. *Apmis* 2007; **115**: 1039–59.
5 Feinberg AP. Phenotypic plasticity and the epigenetics of human disease. *Nature* 2007; **447**: 433–40.
6 Kanai Y, Hirohashi S. Alterations of DNA methylation associated with abnormalities of DNA methyltransferases in human cancers during transition from a precancerous to a malignant state. *Carcinogenesis* 2007; **28**: 2434–42.
7 Kanai Y. Alterations of DNA methylation and clinicopathological diversity of human cancers. *Pathol Int* 2008; **58**: 544–8.
8 Nakagawa T, Kanai Y, Saito Y, Kitamura T, Kakizoe T, Hirohashi S. Increased DNA methyltransferase 1 protein expression in human transitional cell carcinoma of the bladder. *J Urol* 2003; **170**: 2463–6.
9 Nakagawa T, Kanai Y, Ushijima S, Kitamura T, Kakizoe T, Hirohashi S. DNA hypermethylation on multiple CpG islands associated with increased DNA methyltransferase DNMT1 protein expression during multistage urothelial carcinogenesis. *J Urol* 2005; **173**: 1767–71.
10 Nakagawa T, Kanai Y, Ushijima S, Kitamura T, Kakizoe T, Hirohashi S. DNA hypomethylation on pericentromeric satellite regions significantly correlates with loss of heterozygosity on chromosome 9 in urothelial carcinomas. *J Urol* 2005; **173**: 243–6.
11 Kakizoe T, Tobisu K, Takai K, Tanaka Y, Kishi K, Teshima S. Relationship between papillary and nodular transitional cell carcinoma in the human urinary bladder. *Cancer Res* 1998; **48**: 2299–303.
12 Kakizoe T. Development and progression of urothelial carcinoma. *Cancer Sci* 2006; **97**: 821–8.
13 Aleman A, Adrien L, Lopez-Serra L *et al.* Identification of DNA hypermethylation of SOX9 in association with bladder cancer progression using CpG microarrays. *Br J Cancer* 2008; **98**: 466–73.
14 Estecio MR, Yan PS, Ibrahim AE *et al.* High-throughput methylation profiling by MCA coupled to CpG island microarray. *Genome Res* 2007; **17**: 1529–36.
15 Jacinto FV, Ballestar E, Ropero S, Esteller M. Discovery of epigenetically silenced genes by methylated DNA immunoprecipitation in colon cancer cells. *Cancer Res* 2007; **67**: 11481–6.
16 Nielander I, Bug S, Richter J, Giefing M, Martin-Subero JI, Siebert R. Combining array-based approaches for the identification of candidate tumor suppressor loci in mature lymphoid neoplasms. *Apmis* 2007; **115**: 1107–34.
17 Misawa A, Inoue J, Sugino Y *et al.* Methylation-associated silencing of the nuclear receptor I2 gene in advanced-type neuroblastomas, identified by bacterial artificial chromosome array-based methylated CpG island amplification. *Cancer Res* 2005; **65**: 10233–42.
18 Sugino Y, Misawa A, Inoue J *et al.* Epigenetic silencing of prostaglandin E receptor 2 (PTGER2) is associated with progression of neuroblastomas. *Oncogene* 2007; **26**: 7401–13.
19 Tanaka K, Imoto I, Inoue J *et al.* Frequent methylation-associated silencing of a candidate tumor-suppressor, CRABP1, in esophageal squamous-cell carcinoma. *Oncogene* 2007; **26**: 6456–68.
20 Inazawa J, Inoue J, Imoto I. Comparative genomic hybridization (CGH)-arrays pave the way for identification of novel cancer-related genes. *Cancer Sci* 2004; **95**: 559–63.
21 Lopez-Beltran A, Sauter G, Gasser T *et al.* Tumours of the urinary system. In: ed. Eble JN, Sauter G, Epstein JI, Sesterhenn IA. *World Health Organization classification of tumours. Pathology and genetics. Tumours of the urinary system and male genital organs.* Lyon: IARC Press, 2004; 89–157.
22 Illingworth R, Kerr A, Desousa D *et al.* A novel CpG island set identifies tissue-specific methylation at developmental gene loci. *PLoS Biol* 2008; **6**: e22.
23 Arai E, Ushijima S, Fujimoto H *et al.* Genome-wide DNA methylation profiles in both precancerous conditions and clear cell renal cell carcinomas are correlated with malignant potential and patient outcome. *Carcinogenesis* 2009; **30**: 214–21.
24 Manabe D, Saika T, Ebara S *et al.* Comparative study of oncologic outcome of laparoscopic nephroureterectomy and standard nephroureterectomy for upper urinary tract transitional cell carcinoma. *Urology* 2007; **69**: 457–61.
25 Hall MC, Womack S, Sagalowsky AI, Carmody T, Erickstad MD, Roehrborn CG. Prognostic factors, recurrence, and survival in transitional cell carcinoma of the upper urinary tract: a 30-year experience in 252 patients. *Urology* 1998; **52**: 594–601.
26 Harris AL, Neal DE. Bladder cancer – field versus clonal origin. *N Engl J Med* 1992; **326**: 759–61.
27 Maruyama R, Toyooka S, Toyooka KO *et al.* Aberrant promoter methylation profile of bladder cancer and its relationship to clinicopathological features. *Cancer Res* 2001; **15**: 8659–63.
28 Sathyanarayana UG, Maruyama R, Padar A *et al.* Molecular detection of noninvasive and invasive bladder tumor tissues and exfoliated cells by aberrant promoter methylation of laminin-5 encoding genes. *Cancer Res* 2004; **15**: 1425–30.
29 Catto JW, Azzouzi AR, Rehman I *et al.* Promoter hypermethylation is associated with tumor location, stage, and subsequent progression in transitional cell carcinoma. *J Clin Oncol* 2005; **23**: 2903–10.
30 Yates DR, Rehman I, Abbod MF *et al.* Promoter hypermethylation identifies progression risk in bladder cancer. *Clin Cancer Res* 2007; **13**: 2046–2053.
31 Kim EJ, Kim YJ, Jeong P, Ha YS, Bae SC, Kim WJ. Methylation of the RUNX3 promoter as a potential prognostic marker for bladder tumor. *J Urol* 2008; **180**: 1141–5.
32 Maekita T, Nakazawa K, Mihara M *et al.* High levels of aberrant DNA methylation in Helicobacter pylori-infected gastric mucosae and its possible association with gastric cancer risk. *Clin Cancer Res* 2006; **12**: 989–95.
33 Frigola J, Song J, Stirzaker C, Hinshelwood RA, Peinado MA, Clark SJ. Epigenetic remodeling in colorectal cancer results in coordinate gene suppression across an entire chromosome band. *Nat Genet* 2006; **38**: 540–9.
34 Arai E, Ushijima S, Gotoh M *et al.* Genome-wide DNA methylation profiles in liver tissue at the precancerous stage and in hepatocellular carcinoma. *Int J Cancer* 2009; (in press).

35 Stein JP, Lieskovsky G, Cote R *et al.* Radical cystectomy in the treatment of invasive bladder cancer: long-term results in 1,054 patients. *J Clin Oncol* 2001; **19**: 666–75.
36 Gallagher DJ, Milowsky MI, Bajorin DF. Advanced bladder cancer: status of first-line chemotherapy and the search for active agents in the second-line setting. *Cancer* 2008; **113**: 1284–93.
37 Lipponen PK. The prognostic value of basement membrane morphology, tumour histology and morphometry in superficial bladder cancer. *J Cancer Res Clin Oncol* 1993; **119**: 295–300.
38 Scrimger RA, Murtha AD, Parliament MB *et al.* Muscle-invasive transitional cell carcinoma of the urinary bladder: a population-based study of patterns of care and prognostic factors. *Int J Radiat Oncol Biol Phys* 2001; **51**: 23–30.
39 Etoh T, Kanai Y, Ushijima S *et al.* Increased DNA methyltransferase 1 (DNMT1) protein expression correlates significantly with poorer tumor differentiation and frequent DNA hypermethylation of multiple CpG islands in gastric cancers. *Am J Pathol* 2004; **164**: 689–99.

Supporting Information

Additional Supporting Information may be found in the online version of this article:

Fig. S1. Examples of bacterial artificial chromosome (BAC) array-based methylated CpG island amplification (BAMCA) data validation by pyrosequencing.

Table S1. Eighty-three bacterial artificial chromosome (BAC) clones that were able to discriminate noncancerous urothelia obtained from patients with urothelial carcinomas (UCs) (N) from normal urothelia (C) with a sensitivity and specificity of 75% or more.

Table S2. Twenty bacterial artificial chromosome (BAC) clones that were able to discriminate urothelial carcinomas (UCs) in patients who developed recurrence (Pos) from those in patients who did not (Neg).

Table S3. Eleven bacterial artificial chromosome (BAC) clones that were able to discriminate noncancerous urothelia in patients with urothelial carcinomas (UCs) of the renal pelvis or ureter who developed intravesical metachronous UC (Pos) from those in patients who did not (Neg).

Table S4. Genes, CpG islands in the promoter regions, and repeat elements of bacterial artificial chromosome (BAC) clones in Tables S1, S2, and S3.

Table S5. Primer sets for validation study by pyrosequencing.

Table S6. Correlation between smoking history and DNA methylation status in noncancerous urothelia obtained from patients with urothelial carcinomas (UCs) and UCs.

Table S7. Correlation between protein expression levels of DNA methyltransferase (DNMT) 1 and DNA methylation status in noncancerous urothelia obtained from patients with urothelial carcinomas (UCs) and UCs.

Table S8. Correlation between regional DNA hypermethylation on CpG islands and the results of bacterial artificial chromosome (BAC) array-based methylated CpG island amplification (BAMCA) in noncancerous urothelia obtained from patients with urothelial carcinomas (UCs) and UCs.

Please note: Wiley-Blackwell are not responsible for the content or functionality of any supporting materials supplied by the authors. Any queries (other than missing material) should be directed to the corresponding author for the article.

doi: 10.1111/j.1349-7006.2009.01330.x

Cancer Science
The official journal of the Japanese Cancer Association JCA

Establishment of six new human biliary tract carcinoma cell lines and identification of MAGEH1 as a candidate biomarker for predicting the efficacy of gemcitabine treatment

Hidenori Ojima,[1] Daitaro Yoshikawa,[2] Yoshihiro Ino,[1] Hiroko Shimizu,[2] Masashi Miyamoto,[2] Akiko Kokubu,[2] Nobuyoshi Hiraoka,[1] Noriaki Morofuji,[3] Tadashi Kondo,[3] Hiroaki Onaya,[4] Takuji Okusaka,[5] Kazuaki Shimada,[6] Yoshihiro Sakamoto,[6] Minoru Esaki,[6] Satoshi Nara,[6] Tomoo Kosuge,[6] Setsuo Hirohashi,[1,2] Yae Kanai[1] and Tatsuhiro Shibata[1,2,7]

[1]Pathology Division, [2]Cancer Genomics Project, [3]Proteome Bioinformatics Project, National Cancer Center Research Institute, Chuo-ku, Tokyo; [4]Diagnostic Radiology Section, Clinical Trials and Practice Support Division, Center for Cancer Control and Information Services, National Cancer Center, Chuo-ku, Tokyo; [5]Hepatobiliary and Pancreatic Oncology Division, [6]Hepatobiliary and Pancreatic Surgery Division, National Cancer Center Hospital, Chuo-ku, Tokyo, Japan

(Received October 6, 2009/Revised November 25, 2009; December 1, 2009/Accepted December 1, 2009/Online publication January 21, 2010)

The aim of this study was to establish new biliary tract carcinoma (BTC) cell lines and identify predictive biomarkers for the potential effectiveness of gemcitabine therapy. Surgical specimens of BTC were transplanted directly into immunodeficient mice to establish xenografts, then subjected to *in vitro* cell culture. The gemcitabine sensitivity of each cell line was determined and compared with the genome-wide gene expression profile. A new predictive biomarker candidate was validated using an additional cohort of gemcitabine-treated BTC cases. From 55 BTC cases, we established 19 xenografts and six new cell lines. Based on their gemcitabine sensitivity, 10 BTC cell lines (including six new and four publicly available ones) were clearly categorized into two groups, and MAGEH1 mRNA expression in the tumor cells showed a significant negative correlation with their sensitivity to gemcitabine. Immunohistochemically, MAGEH1 protein was detected in three (50%) out of six sensitive cell lines, and four (100%) out of four resistant cell lines. In the validation cohort of gemcitabine-treated recurrence cases, patients were categorized into "effective" and "non-effective" groups according to the RECIST guidelines for assessment of chemotherapeutic effects. MAGEH1 protein expression was detected in two (40%) out of five "effective" cases and all four (100%) "non-effective" cases. We have established a new BTC bioresource that covers a wide range of biological features, including drug sensitivity, and is linked with clinical information. Negative expression of MAGEH1 protein serves as a potential predictive marker for the effectiveness of gemcitabine therapy in BTC. (*Cancer Sci* 2010; 101: 882–888)

Biliary tract carcinoma (BTC) has a poor prognosis, and most cases are diagnosed at advanced stages when patients present with overt symptoms. Previous studies have reported that surgical resection is the only curative treatment for BTC patients,[1–4] and no standard chemotherapy regimens have been established for inoperable cases or cases of recurrence after surgical resection.[5,6] Exceptionally, gemcitabine (2′-deoxy-2′-difluorodeoxycytidine), a deoxycytidine analog with structural and metabolic similarities to cytarabine, has been reported to be clinically effective and is considered a first-line chemotherapy for BTC, although its associated response rates (8–60%) and median overall survival (6.3–16 months) are not satisfactory.[7] It has been reported that both intrinsic and acquired resistance are important factors in the failure of gemcitabine treatment in patients with pancreatic cancer.[8] However, there have been few attempts to clarify the molecular mechanisms of gemcitabine resistance, and no data are currently available for BTC.

One factor preventing better understanding of drug resistance at the cellular and molecular levels in BTC is that only a few BTC cell lines are available for such analyses. Additionally, the construction and utility of an animal experimental model is essential for validating the *in vitro* data for these cell lines, but no such model has been established. Therefore, there is an urgent need to establish BTC cell lines from a wide range of clinical cases and apply them for translational research aimed at connecting basic research with clinical trials. In the present study, we successfully prepared 19 xenograft models from surgically resected BTC samples, and established six new cell lines. Using these new resources, we searched for molecular biomarkers associated with gemcitabine sensitivity. We also validated the efficacy of one candidate molecule, MAGEH1, as a surrogate biomarker of gemcitabine response by immunohistochemical analysis of an additional clinical cohort of gemcitabine-treated BTC.

Materials and Methods

Establishment of xenografts and tumor cell lines. The study included 55 patients with BTC who underwent radical surgery with curative intent at the National Cancer Center Hospital (Tokyo, Japan) between 2005 and 2008. The main tumor nodule was located in the lower, middle, and upper thirds of the extrahepatic bile duct, the hilar bile duct, and intrahepatic area in 4, 11, 2, 4, and 34 patients, respectively. Tumor specimens were transported to the Surgical Pathology department immediately after surgical resection, and tissue in excess of that needed for diagnosis was used for this study. The tumor tissues were washed in physiological saline, cut into small pieces (2–4 mm^3 fragments), then implanted subcutaneously into SCID mice. Congenital athymic female C.B17/Icr-scid(scid/scid) mice (CLEA Japan, Tokyo, Japan), 5–7 weeks old, were bred and housed under specific pathogen-free conditions at the National Cancer Center Research Institute Animal Center. Tumor growth to a size of 1–2 cm after maintaining the animals for 1–2 months was regarded as engraftment, and the tumors were passaged a maximum of three to five times. Xenografts in mice were passaged similarly to the transplantation of surgical

[7]To whom correspondence should be addressed. E-mail: tashibat@ncc.go.jp

doi: 10.1111/j.1349-7006.2009.01462.x

specimens, and the tumors were subjected to cell culture after each passage. For establishment of cell lines, the xenograft tumor tissues were washed in Isozin (Meiji, Tokyo, Japan) and physiological saline, cut into small pieces, then plated into 6 cm dishes containing RPMI medium supplemented with 10% FC), 2 mM L-glutamine, 100 mg/mL streptomycin sulfate, and 100 ID/mL penicillin G sodium. Some surgical specimens were directly subjected to cell line preparation. Contaminating fibroblasts were periodically removed by wiping under microscopic observation. The cells were incubated at 37°C in 5% CO_2 in air, and the medium was changed once or twice a week. A solution of 0.05% trypsin and 0.53 mM EDTA (1×; Gibco™/Invitrogen Corporation, Carlsbad, CA, USA) was used for passaging the cells (1:3 split). Each cell line underwent repeated passage more than 20 times. Established cell lines were implanted subcutaneously into SCID mice to make xenografts for further analyses.

Mice were kept at the Animal Care and Use Facilities of the National Cancer Center (Tokyo, Japan) under specific pathogen-free conditions. All experiments were approved by the Animal Care and Ethics Committee of the National Cancer Center. This study was approved by the Ethical Committee of the National Cancer Center.

Biliary tract carcinoma cell lines obtained from cell banks. Four human BTC cell lines derived from Japanese patients (TKKK, OZ, TGBC24TKB, and HuCCT1) were purchased from Riken Bioresource Center (Tsukuba, Japan) or from the Japanese Collection of Research Bioresources (Osaka, Japan). The TKKK cell line was derived from intrahepatic cholangiocarcinoma, and the OZ, TGBC24TKB, and HuCCT1 cell lines from extrahepatic bile duct carcinoma.

Chemicals. Gemcitabine was obtained from Eli Lilly Pharmaceuticals (Indianapolis, IN, USA). All other chemicals were of analytical grade and commercially available.

Cytotoxicity assays for gemcitabine. The cytotoxicity of gemcitabine for each cell line was assessed by a modified 3-(4,5-dimethylthiazol-2-yl)-5-(3-carboxymethoxyphenyl)-2-(4-sulfophenyl)-2H-tetrazolium, inner salt assay with CellTiter 96 AQueous One Solution Reagent (Promega, Madison, WI, USA). Tumor cells (2000 cells/well) in the exponential growth phase were grown in 96-well plates. Twenty-four hours after plating, the cells were incubated in the presence of each concentration (0 (control)–100 μM) of gemcitabine for another 72 h at 37°C in a humidified atmosphere of 5% CO_2 in air. After treatment, 20 μL CellTiter 96 AQueous One Solution Reagent was dropped into each well in the plates and the absorbance at 490 nm was recorded. Absorbance values were expressed as a percentage of untreated controls, and IC_{50} was calculated.

Gene expression analysis. Total RNA was extracted from 10 BTC cell lines using an RNeasy Micro Kit (Qiagen, Velencia, CA, USA) in accordance with the manufacturer's instructions. The total RNA yields and purity were determined spectrophotometrically by measuring the absorbance of aliquots at 260 and 280 nm. cDNA and Cy3-labeled cRNA were synthesized using a Quick Amp Labeling Kit (Agilent Technologies, Santa Clara, CA, USA). The labeled cRNA probe was hybridized to an oligonucleotide microarray (Whole Human Genome 44K Array; Agilent Technologies) covering more than 41 000 human transcripts. Array hybridization and washing were carried out according to the recommended protocols, and microarrays were scanned using a DNA Microarray Scanner (Agilent Technologies) and analyzed using Gene Spring software (Agilent Technologies).

Quantitative RT-PCR. One microgram of total RNA was converted to cDNA using a Transcriptor First Strand cDNA Synthesis Kit (Roche, Basel, Switzerland) in accordance with the manufacturer's instructions. Quantitative RT-PCR (qRT-PCR) was carried out using LightCycler 480 (Roche) in accordance with the manufacturer's instructions. For standardization of the amount of RNA, expression of GAPDH in each sample was quantified. (Primers are shown in Table S1.)

Mutation analysis of *p53* and *KRAS* genes. Each exon of the *p53* and *KRAS* genes (exons 5–8 of *p53* and exons 1–2 of *KRAS*) was amplified from genomic DNA of each cell line and gel-purified. Direct sequencing was carried out using a BigDye Terminator v3.1 Cycle Sequencing Kit (Applied Biosystems, Foster City, California, USA). (Primers are shown in Table S1.)

Assessment of response to gemcitabine in cases of recurrent BTC. Among the 100 patients who underwent surgery for BTC between September 26, 2003, and October 2, 2007, 34 developed recurrent tumors and received chemotherapy, and were followed for 6 months or longer. Among these patients, 24 who were treated with gemcitabine alone were selected for this study. The mean duration of postoperative follow-up in these 24 patients was 627 days. We further excluded 15 patients from the analysis because: (i) the drug administration period was less than 1 month in three patients; (ii) the diagnosis of tumor recurrence was not consistent between the oncologist and the radiologist in three patients; (iii) we were unable to obtain an accurate judgement of the efficacy of gemcitabine treatment in five patients; (iv) the histological diagnosis was an uncommon type of adenocarcinoma (bile duct cystadenocarcinoma, solid adenocarcinoma, and combined carcinoma) in three patients; and (v) preoperative therapy (radiation therapy) had been carried out in one patient. The effect of chemotherapy was assessed by an oncologist and a radiologist (T.O. and H.O., respectively) in accordance with the RECIST guidelines for assessment of chemotherapeutic effects.[9] None of the patients was judged as showing a complete response or a partial response. The effect of chemotherapy was categorized as "effective" or "non-effective". The "effective" group included patients whose efficacy state was stable disease for 6 months or more during chemotherapy. The "non-effective" group included patients whose efficacy state was stable disease for 5 months or less, or progressive disease during chemotherapy.

Immunohistochemical reactivity of MAGEH1 in human tumor xenografts and surgically resected specimens. Immunohistochemical analysis of MAGEH1 expression on formalin-fixed, paraffin-embedded sections of tumor xenograft tissues and surgical specimens was done using the polymer-based method (Envision+Dual Link System-HRP; Dako, Glostrup, Denmark) in accordance with the manufacturer's instructions. For antigen retrieval, the sections were autoclaved in 10 mM citrate buffer (pH 6.0) at 121°C for 10 min. We used a rabbit anti-MAGEH1 polyclonal antibody (ab64784; Abcom, Cambridge, Massachusetts, USA) at a dilution of 1:500. Staining intensity was independently evaluated by two pathologists (H.O. and T.S.) without knowledge of the clinical data. Using the expression in normal hepatocytes or pancreatic duct epithelial cells as a positive control, we classified cases as MAGEH1-positive when more than 50% of tumor cells were positively stained. If the tumor showed varying degrees of differentiation, staining intensity was evaluated in the area with the most dominant type of differentiation.

Statistical analysis. The unpaired *t*-test was used for assessment of the microarray data. Microarray and qRT-PCR data were analyzed by Pearson's correlation test.

Results

Establishment and characterization of BTC xenografts and cell lines. To establish useful BTC resources, we subcutaneously transplanted 55 BTC samples (4, 11, 2, 4, and 34 cases of lower, middle, and upper thirds of the extrahepatic bile duct carcinoma, hilar bile duct carcinoma, and intrahepatic cholangiocarcinoma, respectively) into 435 immunocompromised (SCID) mice.

Table 1. Clinicopathological features of original biliary tract tumors

Xenograft	Pathological diagnosis of original tumor	Age (years)/Sex	Histologic type	Prognosis (Survival [days])	Cell line
1	CCC	70/F	Adeno, mod	Death (402)	NCC-CC1
2	CCC	71/F	Adeno, mod	Death (175)	NCC-CC3-1/-2
3	CCC	59/M	Adeno, mod	Alive (219)	NCC-CC4-1
4	Middle BDCa	58/F	Adeno, mod	Death (299)	NCC-BD1
5	Lower BDCa	77/F	Adeno, mod	Alive (316)	NCC-BD2
6	Hilar BDCa	48/M	Adeno, well	Death (500)	NA
7	CCC	54/F	Adeno, mod	Death (181)	NA
8	CCC	56/M	Adeno, mod	Death (319)	NA
9	CCC	73/M	Adeno, mod	Death (53)	NA
10	CCC	54/M	Adeno, mod	Alive (655)	NA
11	CCC	45/F	Adeno, mod	Alive (623)	NA
12	CCC	72/M	Muc	Alive (647)	NA
13	Middle BDCa	54/M	Adeno, mod	Alive (535)	NA
14	CCC	69/M	Adeno, mod	Death (174)	NA
15	Hilar BDCa	70/M	Adeno, mod	Alive (355)	NA
16	Middle BDCa	67/M	Adeno, mod	Alive (450)	NA
17	CCC	78/M	Adeno, mod	Alive (299)	NA
18	Middle BDCa	66/F	Adeno, mod	Alive (198)	NA
19	CCC	66/M	Adeno, mod	Death (168)	NA

Adeno, adenocarcinoma; CCC, cholangiocellular carcinoma; F, female; hilar BDCa, hilar bile duct carcinoma; lower BDCa, lower third of extrahepatic bile duct carcinoma; M, male; middle BDCa, middle third of extrahepatic bile duct carcinoma; mod, moderately differentiated; muc, mucinous adenocarcinoma; well, well differentiated; NA, not applicable.

Table 2. Mutation status of *p53* and *KRAS* genes of established novel biliary tract carcinoma cell lines

Cell line	*KRAS* (exons 1–2)		*p53* (exons 5–8)	
	Nucleotide change	Amino acid change	Nucleotide change	Amino acid change
NCC-BD1	G37C	G13C	C457T, A463C,G467C	P153S, T155P, R156P
NCC-BD2	WT	WT	Homozygous deletion	No product
NCC-CC1	G35T	G12V	G524A	R175H
NCC-CC3-1	G35A	G12D	WT	WT
NCC-CC3-2	G35A	G12D	WT	WT
NCC-CC4-1	WT	WT	WT	WT

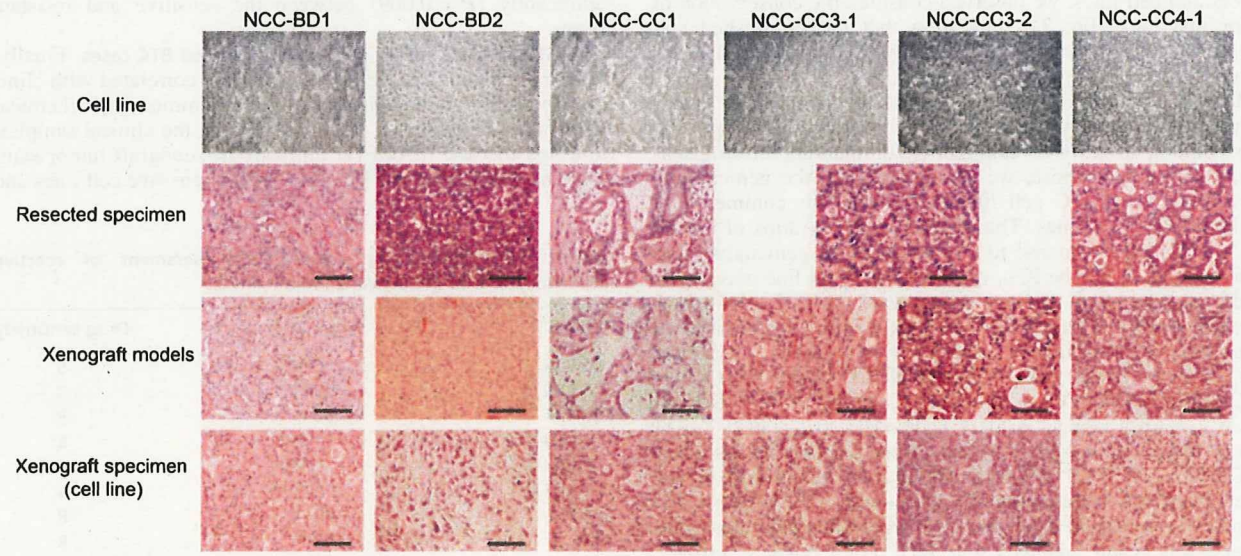

Fig. 1. Cell morphology and tumor histology of primary specimen/xenograft of established new biliary tract carcinoma cell lines. *In vitro* cell morphology and tumor histology (H&E staining) of resected primary specimens, xenografts of primary tumor samples and xenografts of cell lines are shown. Scale line = 200 μm.

doi: 10.1111/j.1349-7006.2009.01462.x

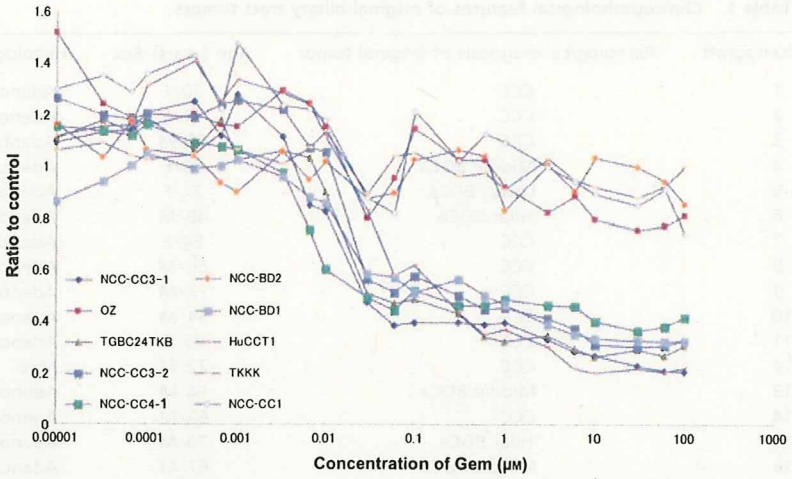

Fig. 2. Sensitivity to gemcitabine (Gem) in 10 biliary tract carcinoma cell lines. Ratio of cell proliferation compared to the control (treated with DMSO) at each concentration (μM) of Gem was plotted. Note that 10 cell lines are clearly segregated into two groups (Gem-sensitive and Gem-resistant) with distinct Gem sensitivity.

Nineteen xenograft models (1, 4, 0, 2, and 12 cases of lower, middle, and upper thirds of the extrahepatic bile duct carcinoma, hilar bile duct carcinoma, and intrahepatic cholangiocarcinoma, respectively) were obtained, and six cell lines including two subclones were established through xenograft models (five cell lines) or directly from a surgical specimen (one cell line). The cell lines were designated as NCC-BD1, NCC-BD2, NCC-CC1, NCC-CC3-1, NCC-CC3-2, and NCC-CC4-1, respectively. Four cell lines were derived from intrahepatic BTC and two from extrahepatic BTC (Table 1). Other clinicopathological features of the patients from whom the cell lines were obtained are summarized in Table 1.

Mutation analysis of the *KRAS* and *p53* genes revealed frequent (3/5, 60%) alterations in them. It also confirmed that these new cell lines were of human origin and that two subclones, NCC-CC3-1 and NCC-CC3-2, shared the same *KRAS* mutation (Table 2). The morphology and histology of the established cell lines and primary tumors, and xenografts of primary tumor and cell lines, are shown in Figure 1. As NCC-BD2 cells were unable to form tumors in mice, we used a cell block of this cell line. Comparing the morphological features between primary tumors and cell lines, we observed considerable conservation of tumor histology (Fig. 1), suggesting that the established cell lines could be considered representative of each original primary.

Classification of 10 BTC cell lines by gemcitabine sensitivity. We then attempted to evaluate whether these new cell lines could be used for revealing novel biomarkers for drug sensitivity. For this purpose, we first determined the gemcitabine sensitivity of 10 BTC cell lines including four commercially available BTC cell lines. The relative survival ratios of the 10 BTC cell lines in response to various doses of gemcitabine are shown in Figure 2. The IC_{50} value for each cell line was calculated, and the results are summarized in Table 3. Interestingly, as can be seen in Figure 2, on the basis of drug sensitivity, we were able to classify these cell lines into two groups: a gemcitabine-sensitive group that included NCC-BD1, NCC-CC3-1, NCC-CC3-2, NCC-CC4-1, HuCCT1, and TGBC24TKB cells (the IC_{50} values being 0.6, 0.03, 0.06, 0.03, 0.2, and 0.03 μM respectively) and a gemcitabine-resistant group that included NCC-BD2, NCC-CC1, TKKK, and OZ cells, whose IC_{50} values were beyond the range of our measurement (>100 μM). As all of the newly established cell lines were from chemotherapy-naïve tumors, this result suggests that BTC cells possess intrinsic molecular mechanism associated with gemcitabine sensitivity.

Significant differences in mRNA expression between groups sensitive and resistant to gemcitabine. To further elucidate the molecular differences between the groups sensitive and resistant to gemcitabine, we investigated the genome-wide mRNA expression in all the cell lines. By comparing the sensitive group with the resistant group, we isolated genes that showed significant differences in expression between the two (Table 4). These included genes associated with cell signaling (*SEC23A*, *RRAS2*, and *BMP8B*) or telomere maintenance (*TERF1*), or genes whose functions were unknown (*NOL10*, *CCDC117*, and *ZSWIM6*). All were candidate biomarkers associated with gemcitabine sensitivity, and among them we focused on MAGEH1 (melanoma antigen family H 1) because: (i) mRNA expression of MAGEH1 in the resistant group was more than five times higher than in the sensitive group; (ii) MAGEH1 is a transmembrane protein that is easily accessible to antibody; and (iii) there was a significant difference in its expression between the two groups ($P = 0.000093$). We then validated the differential expression of MAGEH1 between the two groups by qRT-PCR. As shown in Figure 3, the data for MAGEH1 expression obtained by qRT-PCR, which was normalized with GAPDH expression, was highly correlated with DNA microarray data (coefficient of correlation, 0.847) and also differed significantly ($P = 0.009$) between the sensitive and resistant groups.

MAGEH1 expression in gemcitabine-treated BTC cases. Finally, we tested whether MAGEH1 expression is correlated with clinical response to gemcitabine treatment by immunohistochemical analysis of clinical cases. Before analyzing the clinical samples, we tested the anti-MAGEH1 antibody in xenograft tumor samples. Three cell lines (50%) out of the six sensitive cell lines and

Table 3. Gemcitabine IC_{50} values and assessment of reactive cytotoxicity of biliary tract carcinoma cell lines

Cell line	IC_{50} (μM)	Drug sensitivity
NCC-BD1	0.60	S
NCC-BD2	>100	R
NCC-CC1	>100	R
NCC-CC3-1	0.03	S
NCC-CC3-2	0.06	S
NCC-CC4-1	0.03	S
TKKK	>100	R
OZ	>100	R
Hucct1	0.20	S
TGBC24TKB	0.03	S

R, resistant; S, sensitive.

Table 4. List of genes differentially expressed between gemcitabine sensitive and resistant groups of biliary tract carcinoma cell lines

Gene symbol	Average expression (R)	Average expression (S)	Ratio (R/S)	*P*-value†	Chromosome locus
TIMELESS	1.866235575	0.858141402	2.174741332	1.45E-05	12q12-q13
SEC23A	1.601411675	0.796303448	2.011057064	2.34E-05	14q21.1
MAGEH1	2.100036325	0.397001692	5.289741503	9.28E-05	Xp11.21
NOL10	1.482213925	0.854618707	1.734356987	0.000201766	2p25.1
RRAS2	0.221456871	1.54467481	0.143367956	0.000429397	11p15.2
BMP8B	1.7544659	0.572194878	3.066203432	0.000440394	1p35-p32
TERF1	1.422439425	0.778783987	1.826487767	0.000451224	8q13
SEC23A	1.5599122	0.633786226	2.461259234	0.0004951	14q21.1
CCDC117	1.71272665	0.699035142	2.45012954	0.000557389	22q12.1
C14orf107	0.490823853	1.299093433	0.377820286	0.000632072	14q22.3
ZSWIM6	0.508965063	1.33793895	0.380409781	0.000753833	5q12.1
RPL34	0.52856332	1.102003908	0.479638335	0.000934328	4q25

†Obtained using the unpaired *t*-test. R, resistant group; S, sensitive group.

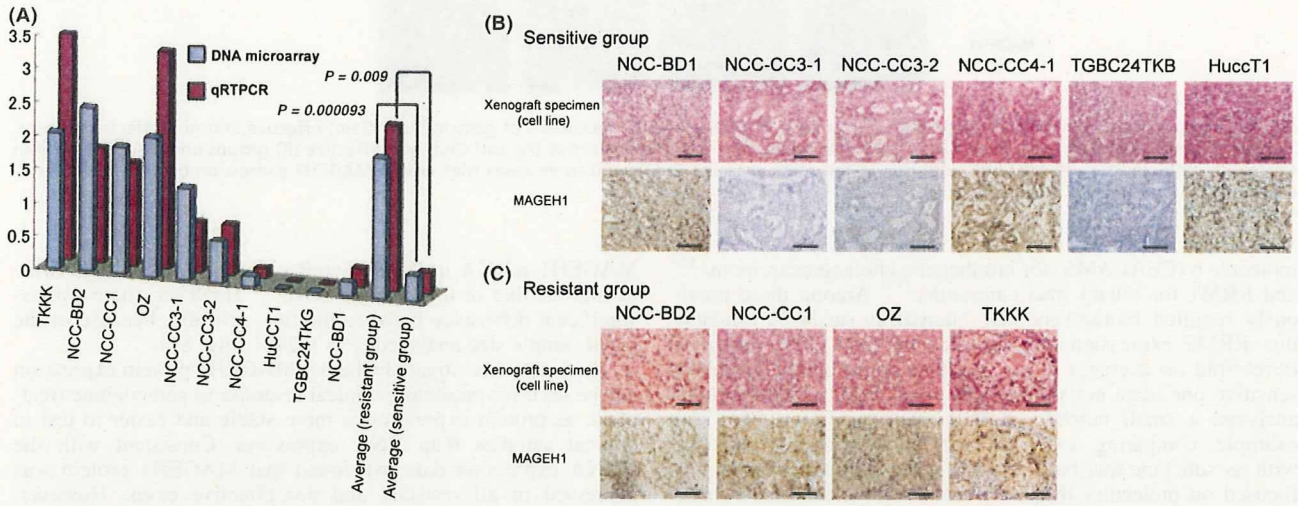

Fig. 3. (A) MAGEH1 mRNA expression in 10 biliary tract carcinoma cell lines. Relative expression of MAGEH1 mRNA compared to GAPDH expression in each cell line was quantified by microarray (blue columns) and quantitative RT-PCR (red columns). MAGEH1 expression was significantly different between gemcitabine (Gem)-sensitive and Gem-resistant groups. (B,C) Immunohistochemical analysis of MAGEH1 protein in xenograft specimens of 10 biliary tract carcinoma cell lines. Tumor histology (H&E staining) of xenograft specimens of cell lines, split into Gem-sensitive (B) and Gem-resistant (C) groups, and MAGEH1 protein expression detected by anti-MAGEH1 antibody in the same area are shown. All three cell lines that lacked MAGEH1 expression belong to the Gem-sensitive group. Scale line = 200 μm.

all four cell lines (100%) in the resistant group were positive for MAGEH1 expression (Fig. 3).

We selected nine recurrent BTC cases treated with gemcitabine alone, which were fully evaluated for drug effects by imaging diagnosis, as described in the "Materials and Methods" section, and whose tumor samples had been sufficiently examined and pathologically diagnosed. After clinical evaluation, we identified five "effective" cases and four "non-effective" cases (Table S2). We examined MAGEH1 protein expression in surgical specimens of the primary tumor in these nine cases. As shown in Figure 4, two (40%) of five "effective" cases were positive, and all four "non-effective" cases (100%) were positive.

Discussion

Elucidation of the molecular mechanisms determining the biological characteristics of cancer cells is one strategy for improving the clinical outcome of BTC patients, but only a few BTC cell lines serving as potent biological tools and animal models with properties resembling those of human cancer have been established. In this study, we succeeded in establishing six novel BTC cell lines including various subtypes and 19 BTC xenograft models after trying 55 cases. Despite carrying out multiple transplantations, we did not observe any marked discrepancy in cell morphology between the original tumors and the cell lines/xenografts, suggesting that this model could be stable and useful for biological studies. Moreover, we were able to fully combine the corresponding clinical information for patients and pathological archive specimens of primary tumors and xenografts for both primary tumors and cell lines with biological data on the cell lines for both basic and preclinical research. To add more clinically relevant functional data, we examined the gemcitabine sensitivities of these cell lines.

Previously, several predictive markers for the effects of gemcitabine chemotherapy have been reported in various types of tumor, including equilibrative nucleoside transporter-1 (hENT1),[10] ribonucleotide reductase subunit M2 (RRM2),[11] and heat shock protein 27 (HSP27)[12] for pancreatic carcinoma, ribonucleotide reductase subunit M1 (RRM1)[13] for non-small-cell lung cancer (NSCLC), hENT1 for ampulla of Vater carcinoma,[14] carcinoembryonic antigen-related cell adhesion

doi: 10.1111/j.1349-7006.2009.01462.x